THE BDM CORPORATION
EDA McLAIN NO. 18-22 WELL
UPSHUR CO., WEST VIRGINIA

VOLUME II
PETROGRAPHY AND GEOCHEMISTRY

Performed by:

Litton Core Laboratories
1300 East Rochelle Blvd.
Irving, TX 75062

December 1986
28G

VOLUME II
PART II

PETROGRAPHY

T A B L E O F C O N T E N T S

S U M M A R Y

The results of a Petrographic Study performed on four (4) shale samples are presented in this report. Thin section analyses and scanning electron microscopy (SEM) with energy dispersive spectroscopy (EDS) were the two analytical techniques employed in this study.

Fabric, Textures,and Sedimentary Structures: These four (4) samples are fissile, planar-laminated shales. A marked parallel alignment is displayed by the elongate grains and clay flakes. The siliciclastic debris includes quartz, feldspar and mica. All four samples are brownish black (5YR 2/1) in color.

Silt and Clay Mineralogy: The relative abundances of silt-size particles, matrix material, authigenic cements, and porosity were determined by point count analyses of 400 points per sample. These analyses show that the silt-size fraction is composed of monocrystalline quartz, polycrystalline quartz, alkali feldspar, plagioclase feldspar, phyllite clasts, chert clasts, muscovite, biotite, and apatite.

Undifferentiated matrix material is the dominant constituent of these four (4) shales. SEM/EDS analyses reveal poorly defined platy clays composed of silicon (Si), aluminum (Al), and potassium (K); these elements indicate an illitic composition for the majority of the matrix material. The presence of iron (Fe), magnesium (Mg), sodium (Na), and calcium (Ca) indicates that the clay species may occur as mixed-layer clay phases such as illite/smectite or illite/chlorite, or may be present as discrete phases. XRD analyses of the clay fraction would be necessary to positively identify these minerals. Minor quantities of kaolinite were detected within this suite of samples. The partially recrystallized detrital clays include mixed-layer illite/smectite and illite.

Organic Material/Residual Hydrocarbon: Abundant, reddish brown to black, nonreflective organic material occurs within the clayey matrix. Further investigation may show these shales to be potential source rocks.

Environment of Deposition: These shales appear to have been deposited under very low energy conditions, probably as suspension deposits.

Authigenic Minerals/Cements: Pyrite, dolomite, and calcite are the dominant authigenic minerals in these samples. Trace quantities of authigenic quartz, feldspar, and a sulphate (gypsum?) are also noted. These authigenic minerals occur as silt-size particle and/or matrix material replacements or as authigenic precipitates. Fairly homogeneously distributed pyrite is the dominant authigenic mineral present.

Porosity: Microporosity, associated with the microporous matrix, is the dominant porosity type present in these four shales. Microporosity cannot be observed during thin section analysis and therefore was not considered in the point count analyses. Minor grain-moldic and possibly artificially induced fracture porosities were also observed.

Reservoir Quality: Based upon pore system geometry, pore volume, and the occurrence of "sensitive" minerals, these shales are classified as poor reservoirs. Enhancement of reservoir quality would occur if the fractures observed in these samples are natural and not artifacts of sampling and sample preparation techniques.

Possible Production Problems and Formation Damage: Potential production problems and formation damage may result if the zones represented by these four shales are improperly treated. These potential problems include the precipitation of insoluble ferric hydroxide gel (pyrite and Fe-bearing clay minerals, such as chlorite), insoluble calcium fluoride precipitation (dolomite, calcite), mobilization of fines (illite, kaolinite, and other fine-size silicates), swelling (smectite, mixed-layer illite/smectite), and scale precipitation (dissolution of sulfates.

Mineralogical Influences on Wireline Log Responses: Optimistic "effective" porosity values may be derived from the neutron density log due to "bound" water associated with the microporous matrix material and the presence of hydrous minerals (minor). Density values may be higher than anticipated, depending on the matrix material composition and the presence of abundant pyrite. Suppression of the resistivity log may occur due to the abundance of pyrite. The gamma ray log response is expected to be characteristic of a shale.

I N T R O D U C T I O N

Four (4), moderately consolidated samples were received by the Reservoir Geology/Petrographic Services Group of Core Laboratories, Inc., in Dallas, Texas on October 2, 1986. The client company, Petrophysical Services, Inc., requested that a Core Research including detailed Thin Section Petrography and Scanning Electron Microscopy (SEM) with Energy Dispersive Spectroscopy (EDS) be performed on each sample. These samples are numbered 28G-1 through 28G-4.

The objectives of this study include the determination of:

1) Megascopic features, fabrics, and textures;

2) Silt, matrix, cement, and clay compositions and abundances;

3) Types, amounts, and distribution of porosity;

4) Estimation of reservoir quality;

5) Occurrences of potential problem minerals;

6) Possible mineralogic effects on completion, production, enhanced recovery, and wireline logs; and

7) General recommendations to circumvent or mitigate these possible difficulties.

A list of the types of analyses performed and the information provided by each of these analyses is cited below.

Petrographic Analysis by Thin Section provides the following information:

1) Textural information (sorting, packing, grain-size, fabric, lithification);

2) Framework-grain mineral identification and quantification (based on modal point count analyses of 400 points per sample);

3) Presence, location, distribution, and identification of matrix material;

4) Identification, quantification, and distribution of authigenic cementing agents;

5) Identification, quantification, and distribution of the different types of pores present; and

6) Reservoir quality evaluation.

Examination by Scanning Electron Microscopy reveals the following:

1) Low magnifications give textural information concerning lithification, sorting, grain-size, distribution of matrix material, and distribution of pores;

2) Higher magnifications reveal the morphology (detrital or authigenic) and location of the "sensitive" minerals present;

3) Distribution and types of authigenic cements present;

4) Identification of clay minerals, cements, and framework grains by use of EDS; and

5) Reservoir quality evaluation.

D I S C U S S I O N

A Petrographic Study, including thin section petrography and scanning electron microscopy (SEM) with energy dispersive spectroscopy (EDS) analysis, was performed on four (4) whole-core shale samples. These four (4) samples are designated as 28G-1, 28G-2, 28G-3, and 28G-4. An interpretation of the data derived from these analyses is presented in the following discussion.

FABRIC, TEXTURES, AND SEDIMENTARY STRUCTURES

Megascopic and microscopic examination of these samples reveal four (4) planar-laminated, fissile shales (Picard, 1971). Color analyses show all four samples to be brownish black (5YR 2/1; Goddard et al., 1980). Parallel alignment of the platy and elongate minerals occurred during the compactional phase of diagenesis which resulted in the formation of the planar laminae and fissile layering. Minor disruption of the planar laminae are occasionally observed where authigenic minerals have precipitated. No evidence of burrowing or other infaunal activity was observed.

The silt-size particles present in all four samples, consist of angular to rounded and elongate to equant quartz, feldspar, apatite, and mica. This clastic detritus is present in pockets or, more commonly, as heterogeneously disturbed particles set in an abundant clayey matrix. Floating particle contacts predominate; however, point and line contacts are observed where pockets of silt-size particles occur.

SILT AND CLAY MINERALOGY

A point count analysis of 400 points (Table 2), was performed on each of the four (4) samples to determine relative abundances of silt, clay, authigenic minerals, and porosity.

The following minerals were identified during point count analyses: monocrystalline quartz, polycrystalline quartz, alkali feldspar, plagioclase feldspar, phyllite clasts, chert clasts, muscovite, apatite, and biotite. These particles represent from 13.5 percent (28G-2) to 20.8 percent (28G-4) of the samples.

The monocrystalline quartz is most commonly nonvacuolized, occurring as heterogeneously distributed, angular to rounded particles. Polycrystalline quartz particles, consisting of interlocking quartz crystals, are widely scattered throughout the matrix. Both untwinned and twinned feldspars were observed in all four samples. Spindle-twinned alkali feldspar is the most frequently observed feldspar. Lesser quantities of albite-twinned plagioclase feldspar and untwinned feldspar were observed. Rock fragments consisting of phyllite (28G-1) and chert clasts (28G-3) were rarely noted. Moderate quantities of

muscovite flakes displaying parallel alignment to the fissile-layering are present in these sample. Trace (28G-4) to 0.8 percent (28G-2) of apatite particles were noted. It is unclear whether the apatite is present as detrital particles or as collophane, a biogenically derived apatite.

No spores or fossil fragments were observed during these analyses. Complete replacement of the spores and/or fossil fragments by authigenic phases, such as pyrite or carbonate minerals, may explain their absence. The thin section photomicrographs of Samples 28G-1 (Plate 1) and 28G-3 (Plate 2A) show several "elongate" aggregates of carbonate minerals. These may represent compacted and replaced spores. The detrital clayey matrix material (categorized as undifferentiated matrix material; Table 2) and orthomatrix are the dominant constituents of these samples, ranging from 42.3 percent (28G-1) to 61.0 percent (28G-2) of the total sample. Preferred orientation, a compactional feature, is displayed by the detrital clay fractions. Aggregate extinction of the clay minerals is noted when the thin sections are viewed under crossed polarizers.

Analyses by scanning electron microscopy (SEM) and energy dispersive spectroscopy (EDS) reveal that undifferentiated, detrital to partially recrystallized, clay minerals are the dominant constituents of these four shales.

The clay minerals (Plates 5B, 8A, 10, 12A) are most commonly observed overlapping the platy detrital clays. EDS analyses of these clays show that silicon (Si), aluminum (Al), and potassium (K) are the dominant elements present. The predominance of these elements indicates clay minerals of illitic composition. Lesser quantities of iron (Fe), sodium (Na), and calcium (Ca) were also detected as constituents of the clayey matrix. The presence of these elements may indicate that a fraction of the clays comprising these samples may be mixed-layer illite/ smectite, smectite, mixed-layer illite/chlorite, and/or kaolinite. These clay minerals may be present as discrete phases or as mixed-layer clays. It would be necessary to perform X-ray diffraction (XRD) analyses on the clay fraction of all four shales to accurately determine the composition of the clay minerals.

Some morphological characteristics indicative of certain clay minerals were observed during SEM analyses. A clay closely resembling mixed-layer illite/smectite is present in Sample 28G-4 (Plate 12A). Wispy lath-like fibrils characteristic of illite are noted in Sample 28G-3 (Plate 10A). Silicon (Si) and aluminum (Al) only were detected in some of the particle-coating clay flakes in Sample 28G-1 (Plate 5B). The presence of silicon (Si) and aluminum (Al) only, are indicative of a clay mineral of the kaolinite family.

Finely disseminated pyrite and organic material are intermixed with the clayey matrix materials.

ORGANIC MATERIAL/RESIDUAL HYDROCARBON

A reddish-brown to black, organic material/residual hydrocarbon occurs throughout the matrix. This material is nonreflective when viewed under reflected light and translucent to opaque when viewed using transmitted light.

ENVIRONMENT OF DEPOSITION

These four shale samples were most likely deposited under very low energy conditions, such as suspension deposition. The presence of silt-size debris indicates that higher-energy conditions prevailed occasionally.

AUTHIGENIC MINERALS/CEMENTS

Authigenic minerals, including pyrite, dolomite, calcite, and a sulphate mineral (gypsum?), represent from 22.0 percent (28G-4) to 30.0 percent (28G-1) of these samples, as derived by point-count analyses (Table 2). These authigenic minerals consist of both replacement minerals and/or authigenic precipitates.

Pyrite is the dominant authigenic phase present in these shales. It occurs primarily as a replacement of the matrix material. Pyritohedrons and framboidal pyrite (Plate 12B) occur in all samples. The pyrite is finely disseminated throughout the matrix. Where pyrite growth has been extensive, disruption of the fissile layering is observed.

The carbonate minerals, comprised primarily of dolomite with lesser amounts of calcite, are heterogeneously distributed throughout these samples (Plate 1B, 2B, 3B, 6B). The dolomite fraction occurs as subhedral to euhedral crystals. EDS analyses indicate that the dolomite is iron-rich. Calcite is present as euhedral crystals and as anhedral crystals within crystalline aggregates. Both the dolomite and the calcite replace the matrix material and the silt-size particles including spores(?).

Trace quantities of a sulphate mineral (gypsum?) were noted during the SEM/EDS analyses of Sample 28G-3 only. SEM/EDS analyses also revealed minor quantities of authigenic quartz (Plate 11B) and feldspar (Plate 12B).

POROSITY

The dominant porosity type present in these four (4) shale samples is microporosity; lesser quantities of fracture and grain-moldic porosity were also observed. Abundant microporosity is associated with the clayey matrix (Plates 5-12). Micropores

are defined as those pores ranging from 0.5-1.0 microns in diameter. These micropores are considered to represent ineffective porosity. Microporosity can be neither detected nor quantified during thin section analyses and, therefore, is not considered in the tabulation of the point-count data.

Fracture porosity is present in all four samples; however, the fractures observed during thin section analyses appear to be the result of sample preparation.

Minor quantities of grain-moldic porosity were observed in Samples 28G-1 and 28G-3 only.

A significant reduction in porosity occurred during the compactional phase of diagenesis and, to a lesser extent, where authigenic minerals have precipitated. The reduction of porosity during the compactional stage of diagenesis was the most important factor in porosity reduction. Some enhancement of porosity has occurred where unstable mineral phases have undergone dissolution; however, overall porosity has been very significantly reduced.

RESERVOIR QUALITY

The determination of reservoir quality is based upon;

1) pore network configuration;

2) porosity values derived by point-count analyses; and

3) the presence and locations of "sensitive" minerals that could cause formation damage or reduce production.

Very poor reservoir quality characteristics are shown by these four shales, as based upon the above-listed characteristics. If the fractures noted during these analyses are natural, then reservoir quality would be greatly improved.

POSSIBLE PRODUCTION PROBLEMS AND FORMATION DAMAGE

The physicochemical characteristics of certain "sensitive" minerals and/or locations of these minerals may pose potential production problems, or if improperly treated may cause formation damage. The "sensitive" minerals observed in these samples and the problems commonly associated with these minerals are listed below.

Illite Family

Illite is a three-layered, hydrated silicate containing potassium, silicon, and aluminum. Authigenic illite generally occurs as crenulated sheets with lath-like projections, and can create

high microporosity and high irreducible water saturations. In the presence of high flow rates, the lath-like projections can break off and migrate to pore throats, resulting in a reduction of permeability. Illite may be dissolved with a weak mixture of HCl/HF acids.

Pyrite

Iron-rich pyrite is sensitive to acids and oxygenated waters. Therefore, an iron-chelating agent and oxygen scavenger should be introduced with any acid stimulations to inhibit the precipitation of pore-plugging ferric-hydroxide gel.

Smectite (including Mixed-Layer Illite/Smectite)

Smectite is a water-sensitive alumino-hydrosilicate structurally similar to mica but with weaker bonds between the layers. Exposure to fresh water causes swelling which can result in a reduction of permeability. Swelling problems can be overcome by the use of oil-based or potassium chloride drilling, completion, and stimulation systems.

Kaolinite Family

Kaolinite is a two-layered, hydrated alumino-silicate. The loose attachment of pseudohexagonal platelets of authigenic kaolinite to host grains can result in clay migration to pore throats, particularly if high flow rates are achieved. Exposure to strong acids also may enhance migration. The introduction of a clay stabilizer after stimulation with hydrochloric (HCl) and hydrofluoric (HF) acids should inhibit the migration of authigenic kaolinite.

Carbonate Minerals

Dissolution of calcite, and to a lesser extent dolomite and ankerite, in HF acid can lead to the precipitation of insoluble calcium fluoride. Therefore, these carbonates should be dissolved first with HCl acid before treatment with HF or fluoboric acid. Iron-rich siderite and ankerite require the introduction of an iron-chelating agent with any acid stimulations to inhibit the precipitation of ferric hydroxide. Preflushing with HCl is required with any acid stimulations for reservoirs in which carbonates are present.

Fine-grained silicates

The reaction of HF acid with fine, silicate minerals can result in the precipitation of colloidal silica. The extent of this precipitation depends upon HCl/HF concentration and the amount of clay in the reservoir rock.

Gypsum/Anhydrite

These calcium sulphate minerals will dissolve upon contact with fresh water. A fluid with high brine content should be used in order to prevent dissolution of this mineral.

MINERALOGICAL INFLUENCES ON WIRELINE LOG RESPONSES

The presence of certain minerals due to their physical characteristics, chemical compositions, and/or abundances may influence wireline log responses. Erroneous assessments of reservoir quality may be derived from affected log responses.

The following logs may be affected:

1) Neutron Porosity Log: Hydrous minerals, such as clays and gypsum, and "bound" water occurring in conjunction with micropores, will be recorded as part of the total formation porosity. Thus, porosity values derived from the neutron porosity log are anticipated to be more optimistic than effective porosity for fluid-flow considerations.

2) Resistivity Log: Semi-conductive pyrite, an important constituent in all these shale samples, may cause resistivity suppression due to its high conductivity. Water saturation (S_w) values calculated from resistivity logs, therefore, may not accurately reflect true, ambient water saturations.

3) Density Log: Estimation of porosity values from density logs are usually based on an assumed grain density of 2.65g/cc (sandstone). However, significant quantities of pyrite (4.95-5.03g/cc) suggest that overall grain density may be increased and thus, if uncorrected, computed density porosity values may be higher than expected.

4) Gamma Ray Log: Due to the presumed, fairly high illite content, these samples are anticipated to yield gamma ray responses characteristic for shales.

A N A L Y T I C A L P R O C E D U R E S

For the Scanning Electron Microscopy/Energy Dispersive Spectroscopy (SEM/EDS) Study, the samples are broken to form fresh surfaces. Each sample is then mounted on an aluminum stub and coated with a thin film of gold-palladium (Au-Pd) alloy using an ISI-PS2 Coating Unit. The SEM photomicrographs are secondary electron images taken with a Polaroid camera attached to an ISI-SX-40 Scanning Electron Microscope operating at 20kV. Qualitative elemental data of selected phases observed during the SEM study are obtained through the use of an interfaced PGT System III Energy Dispersive Spectroscopy Unit equipped with Si(Li) detector. Recognition of the authigenic clay minerals is based on the criteria proposed by Wilson and Pittman (1977).

The sample fractions are prepared for Thin Section Analysis by first impregnating the sample with epoxy to augment sample cohesion and to prevent loss of material during grinding. A blue dye is added to the epoxy to highlight the porosity. Each sample is mounted on a glass slide, and then cut and ground in water to an approximate thickness of 30 microns. Samples containing known water-soluble phases are prepared using odorless kerosene. Prepared thin sections are subsequently stained for calcium (Alizarin Red-S stain), iron (potassium ferricyanide stain), and potassium (sodium cobaltinitrate stain) as necessary. The thin sections are analyzed using standard petrographic techniques. Modal analyses of the sections are performed by the point-count method (400 points/sample) using a Swift Model F Automatic Point Counter. Mineralogy and porosity percentages are calculated from raw point count data, using a special point count routine developed by Core Laboratories, Inc. Actual totals may deviate slightly from 100 percent due to computer rounding. Picard's (1971) classification scheme is used for mudrock samples.

R E F E R E N C E S

Goddard, E.N., P.D. Trask, R.K. DeFord, O.N. Rove, J.T. Singewald, and R.M. Overbeck, 1980, Rock Color Chart: Geological Society of America, Boulder, Colorado.

Picard, M.D., 1971, Classification of fine-grained sedimentary rocks: Journal of Sedimentary Petrology, Volume 41, p. 179-193.

Wilson, M.D. and E.D. Pittman, 1977, Authigenic clays in sandstones: recognition and influence of reservoir properties and paleoenvironmental analysis: Journal of Sedimentary Petrology, Volume 47, p. 3-31.

TABLE 1
THIN SECTION ANALYSES: TEXTURE

Sample Number:	28G-1	28G-2	28G-3
Name (Picard, 1971):	Shale	Shale	Shale
Color of Hand Sample (Goddard, et al., 1980):	Brownish black (5 YR 2/1)	Brownish black (5 YR 2/1)	Brownish black (5 YR 2/1)
Lithification:	Moderate	Moderate	Moderate
Fabric and Textures:	Well-developed alignment of elongate and/or compacted particles	Well-developed alignment of elongate and/or compacted particles	Well-developed alignment of elongate and/or compacted particles
Sedimentary Structures:	None	None	None
Fissility:	Well-developed	Well-developed	Well-developed
Porosity Types:	Grain-moldic	No visible porosity	Grain-moldic

TABLE 1 (Cont'd)
THIN SECTION ANALYSES: TEXTURE

Sample Number:	28G-4
Name (Picard, 1971):	Shale
Color of Hand Sample (Goddard, et al., 1980):	Brownish black (5 YR 2/1)
Lithification:	Moderate
Fabric and Textures:	Well-developed alignment of elongate and/or compacted particles
Sedimentary Structures:	None
Fissility:	Well-developed
Porosity Types:	No visible porosity

TABLE 2
THIN SECTION ANALYSES: COMPOSITION

Sample Number	28G-1	28G-2	28G-3	28G-4
FRAMEWORK GRAINS	14.8	13.5	17.0	20.8
Quartz	8.8	10.0	10.3	13.5
Monocrystalline	8.8	10.0	10.0	13.0
Polycrystalline	0.0	0.0	0.3	0.5
Feldspar	1.0	0.3	0.3	1.5
Alkali Feldspar	0.5	0.3	0.3	1.0
Plagioclase	0.5	0.0	0.0	0.5
Rock Fragments	0.3	0.0	0.3	0.0
Metamorphic	0.3	0.0	0.0	0.0
Phyllite	0.3	0.0	0.0	0.0
Sedimentary	0.0	0.0	0.3	0.0
Chert	0.0	0.0	0.3	0.0
Accessory Grains	4.5	3.0	6.3	5.8
Muscovite	4.0	2.3	6.0	5.5
Apatite	0.5	0.8	0.3	0.0
Biogenic Materials	0.3	0.3	0.0	0.0
Fossil Fragments	0.3	0.3	0.0	0.0
MATRIX	55.0	63.5	55.8	57.3
Orthomatrix	12.8	2.5	1.3	0.5
Undifferentiated	42.3	61.0	54.5	56.8
AUTHIGENIC CEMENTS	30.0	23.0	27.0	22.0
Dolomite	2.5	1.0	3.0	1.8
Pyrite	27.5	22.0	24.0	20.3
POROSITY	0.3	0.0	0.3	0.0
Dissolution	0.3	0.0	0.3	0.0
Grain Moldic	0.3	0.0	0.3	0.0
Intragranular	0.0	0.0	0.0	0.0
TOTAL	100.0	100.0	100.0	100.0

T A B L E 3

POTENTIAL FORMATION DAMAGE FROM MINERAL COMPONENTS

Magnitude of Potential Problem	"Sensitive" Mineral	Potential Problem	Avoid Using	Use	Treatments to Eliminate Problems
****** = Maximum * = Minimum					
****	Illite	migration of fines/ micro-porosity "mushing"	high flow rates/ fresh-water systems	low flow rates/KCl or hydro-carbon systems	acidize with HCl/ HF and use correct pre- and after-flushes
****	Pyrite	iron-hydroxide precipitate, sulphate production	oxygen rich systems, fluids containing Ca^{+2}, Sr^{+2}, Ba^{+2}	acid systems, oxygen scavengers	acidize with HCl/ HF and use suit-able chelating agent
***	Smectite (including Mixed-Layer Illite/Smectite)	swelling	fresh-water systems	KCl or hydrocarbon systems	acidize with HCl/ HF and use correct pre- and after-flushes
***	Kaolinite	migration of fines	high flow rates/high transient pressures	low flow rates/low transient pressures	use a clay stabilizer
**	Fine-grained silicates	silicon	concentrated HF	dilute HF	acidize with HCl/ HF and use correct pre- and after-flushes
*	Sulphates (gypsum/ anhydrite)	dissolution	fresh water	fluids with high brine	introduce fluids with high brine content content

THIN SECTION

PHOTOMICROGRAPHS AND DESCRIPTIONS

The scale of the photomicrographs in each Plate is a function of the magnification:

40X: Horizontal width of the photomicrograph represents 3.175mm.

200X: Horizontal width of the photomicrograph represents 0.635mm.

Core Research, Inc. File: 186216

Sample Number: 28G-1

Plate 1A

A fissile, planar-laminated shale is shown in this low-magnification image. The silt-size detritus is composed of quartz, alkali feldspar, phyllite clasts, muscovite flakes, apatite, and fossil fragments. A deep brownish black, nearly opaque, matrix material consisting of clay, finely divided pyrite, organic material, and clay-size quartz and feldspar particles occupies much of the field of view. Abundant framboidal pyrite and subhedral to euhedral dolomite crystals are the authigenic minerals observed in this sample. The fracture porosity (blue epoxy) shown in this view appears to be the result of sample preparation. (40X, plane-polarized light)

Plate 1B

A detailed view of the matrix material is provided in this high-magnification photomicrograph. The opaque material (B1, F5, G12, J14) consists of pyrite (E12, J5, pyritized organic material?) and organic material. Detrital to slightly recrystallized, clayey matrix material displays a golden brown hue (F13, J14). Authigenic dolomite crystals (D2, E8, F10) occur as matrix-replacive minerals and authigenic precipitates. An altered, compacted spore(?) can be observed at D7. The siliciclastic debris shown floating in the matrix material consists of quartz, feldspar, and muscovite. (200X, plane-polarized light)

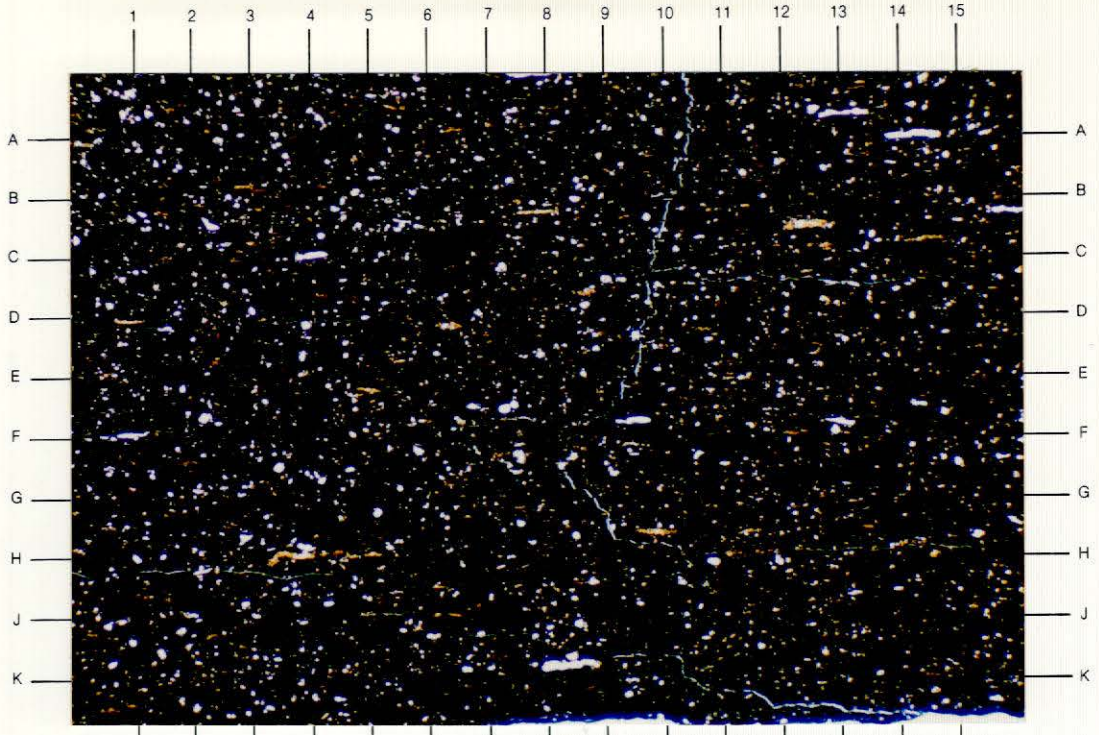

A

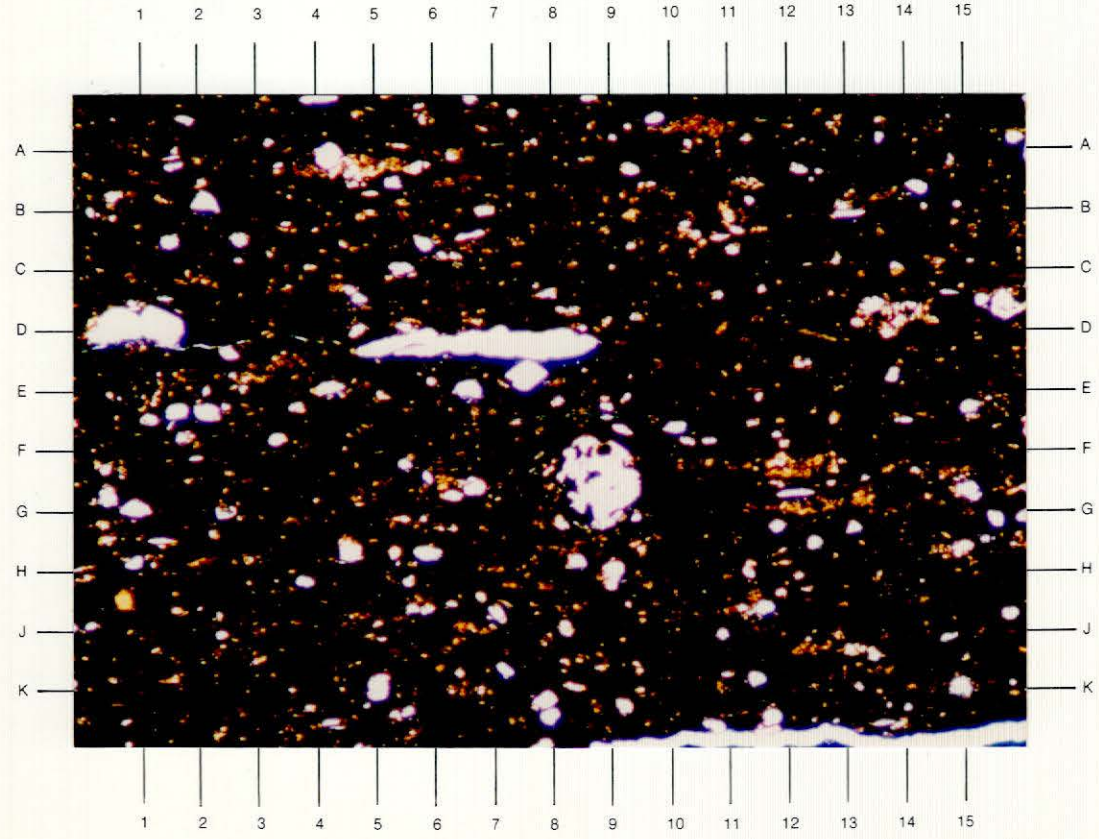

B

CORE LABORATORIES, INC.

Reservoir Geology/Petrographic Services

Core Research, Inc. File: 186216

Sample Number: 28G-2

Plate 2A

This general view of the sample reveals a fissile, planar-laminated shale. Silt-size particles of quartz, feldspar, and muscovite fleck the deep brown to black matrix material, the dominant constituent of this shale. The matrix material consists primarily of pyrite, detrital to partially recrystallized detrital clay, and clay-size quartz and feldspar particles. Heterogeneously distributed dolomite crystals and numerous, fairly homogeneously distributed pyrite crystals are the most abundant authigenic minerals cementing this sample. The fractures present in this sample (blue-dyed epoxy) are artifacts of sample preparation. (40X, plane-polarized light)

Plate 2B

The abundance of opaque material in this sample is clearly evident in this high-magnification image. Fissile clay layers (golden to orangish brown) are often disrupted by the growth of framboidal pyrite aggregates (E5). Dolomite can be observed at E9 and J12. Silt-size particles (A7, D14, J9-10) dot the matrix material. (200X, plane-polarized light)

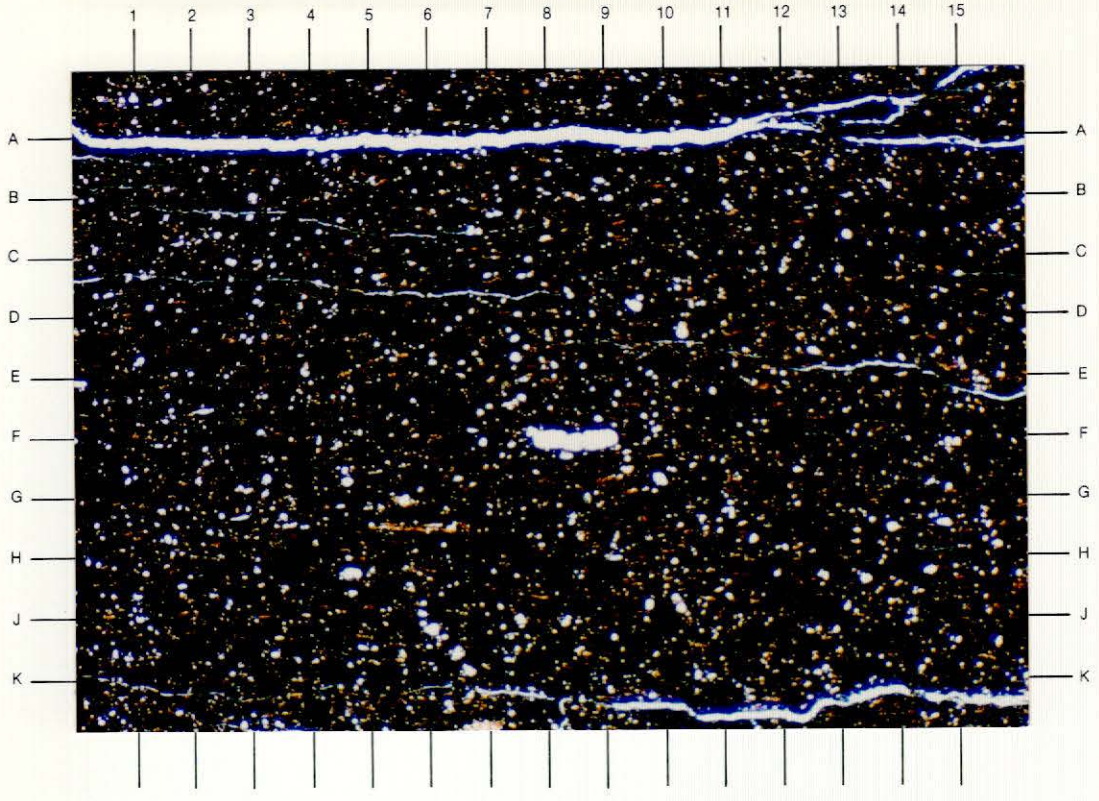

A

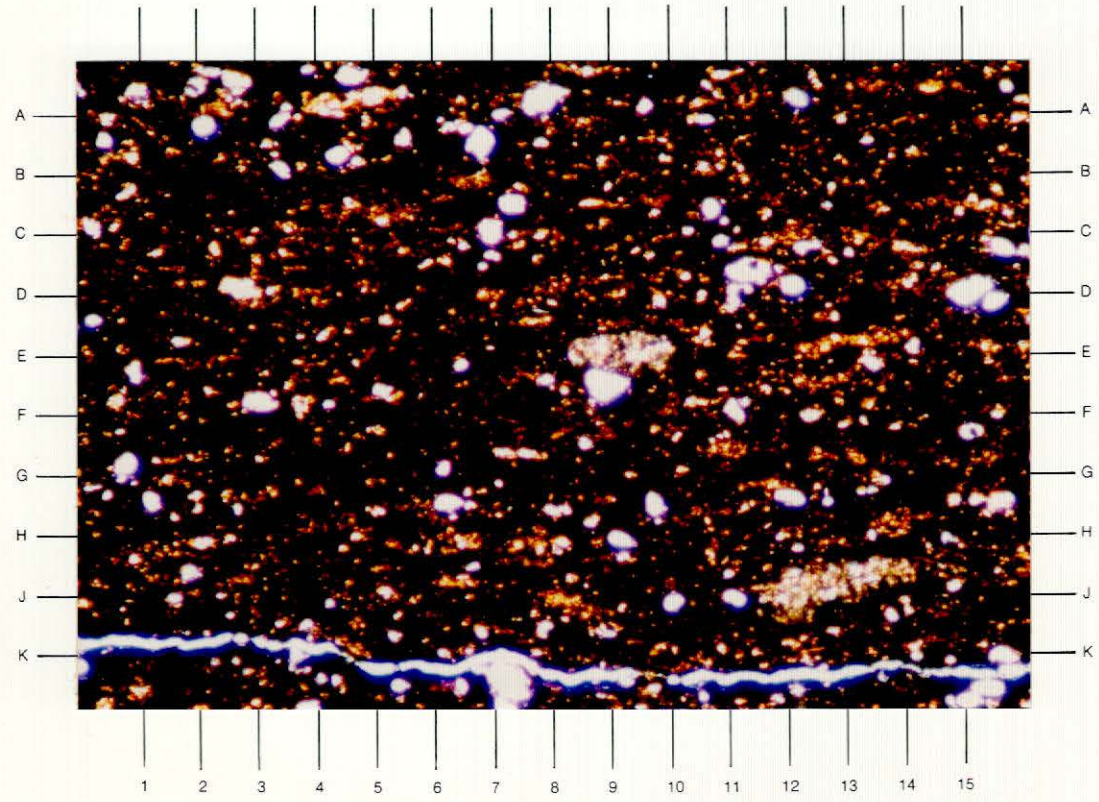

B

CORE LABORATORIES, INC.

Reservoir Geology/Petrographic Services

Core Research, Inc. File: 186216

Sample Number: 28G-3

Plate 3A

This low-magnification view of a shale shows numerous silt-size particles of quartz, feldspar, and muscovite suspended in a deep brown matrix. This brown matrix is composed of detrital to partially recrystallized clays and finely divided aggregates of pyrite and organic material. Authigenic pyrite and dolomite partially replace the matrix material and silt-size particles. The fractures that occur at E6 and on the uppermost edge of this view were induced during sample preparation. (40X, plane-polarized light)

Plate 3B

The nearly black color of the matrix in this high-magnification photomicrograph is indicative of the high pyrite content present in these shales. Detrital to partially recrystallized, clayey matrix material is present as the golden to orangish brown, anisotropic material (E5). Silt-size (A12, F13) quartz and feldspar particles fleck the matrix material. A dolomite aggregate occurs at F8. (200X, plane-polarized light)

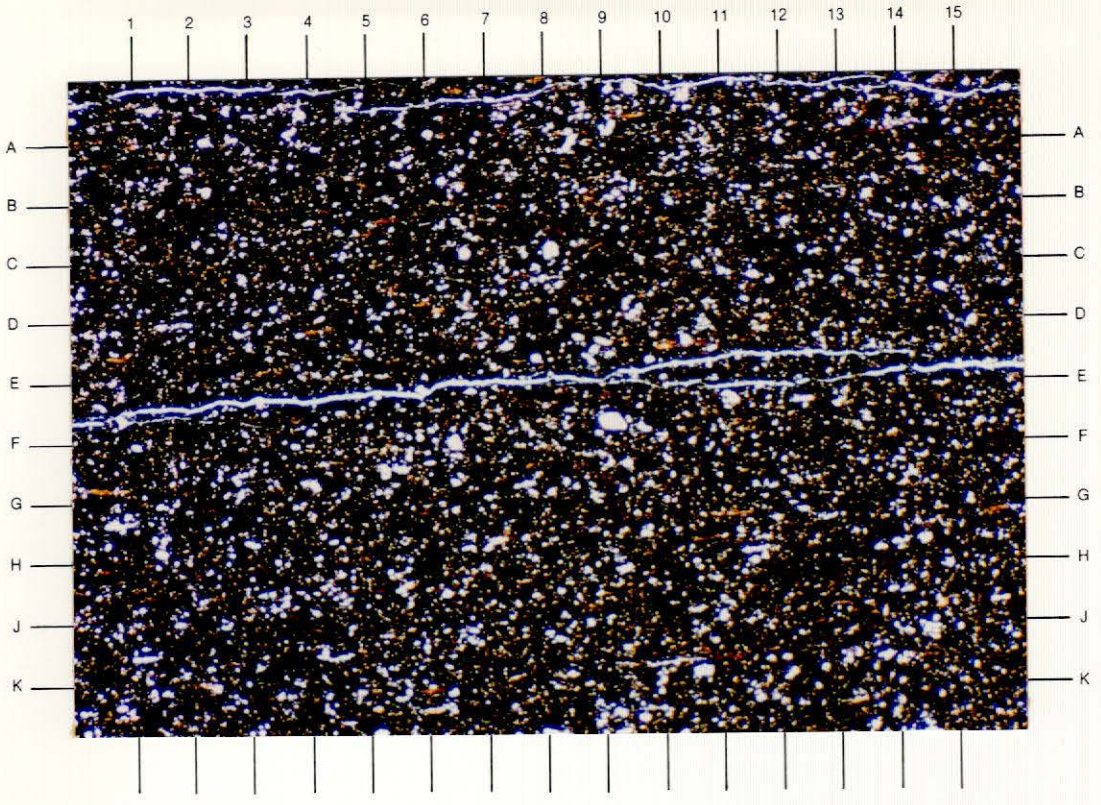

A

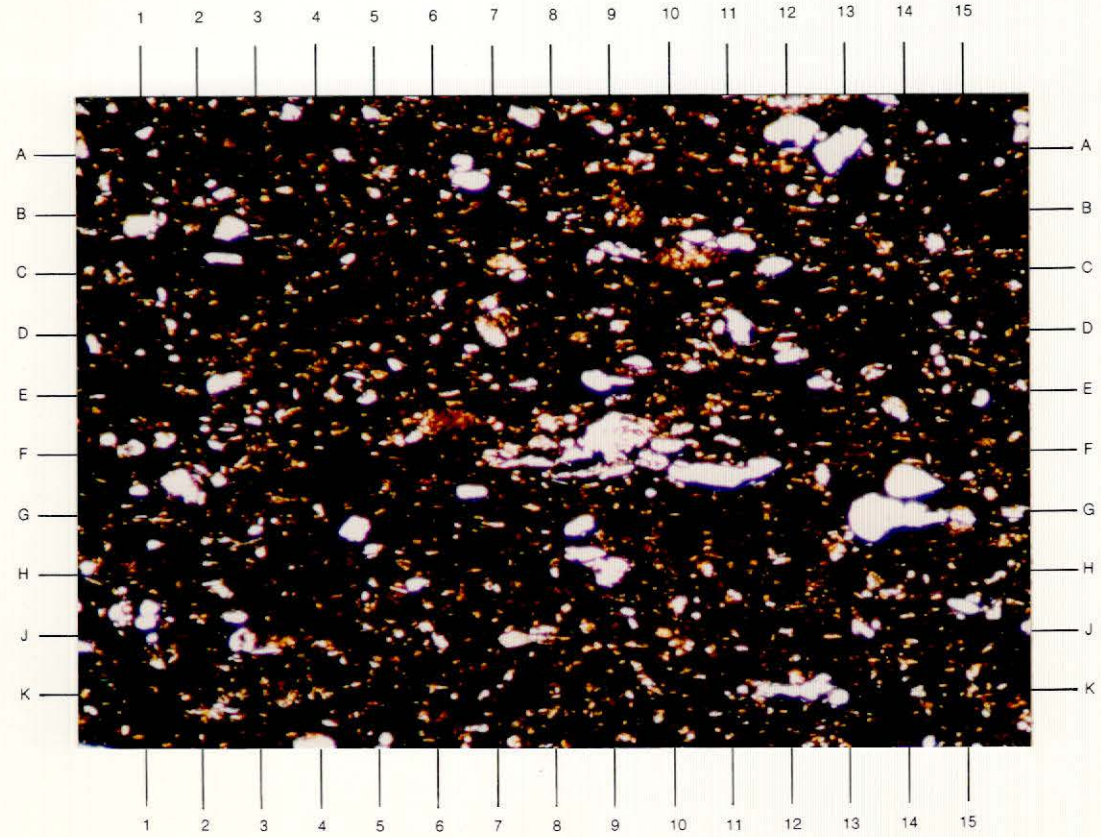

B

CORE LABORATORIES, INC.

Reservoir Geology/Petrographic Services

Core Research, Inc. File: 186216

Sample Number: 28G-4

Plate 4A

A low-magnification image reveals a fissile, planar-laminated shale. Silt-size particles of quartz, feldspar, and muscovite float in the deep brown to black matrix. The matrix material consists of clays, organic material, and finely divided pyrite. Authigenic minerals include pyrite, dolomite, and calcite. The open fractures (blue epoxy) present in this view are a result of sample preparation techniques. (40X, plane-polarized light)

Plate 4B

The abundance of opaque matrix material is highlighted in this detailed image of the sample. This opaque matrix consists of organic material and pyrite (pyritized organic material?). Silt-size quartz, feldspar, and muscovite particles are suspended in this deep brown to black, clay-rich matrix. Partially recrystallized and/or detrital clays (A1, G4), which are golden brown in color, fleck this sample. The minute fracture present at F-G15 is an artifact of sample preparation. (200X, plane-polarized light)

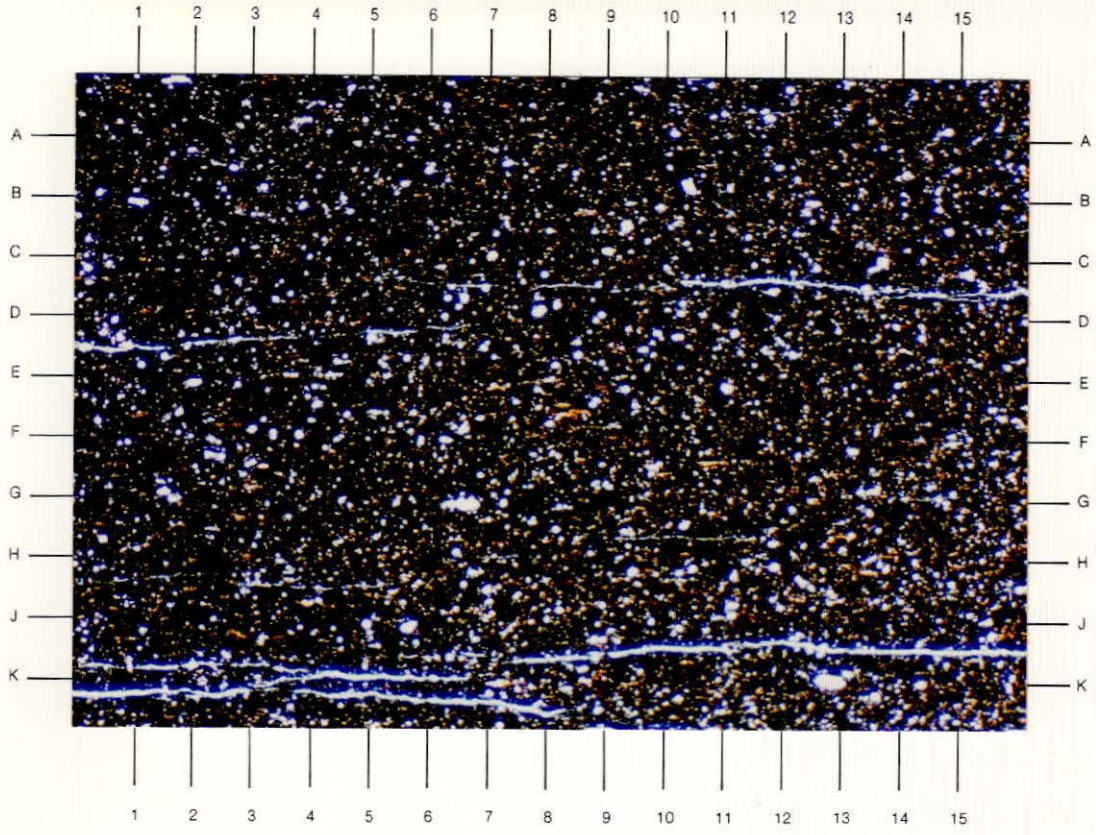

A

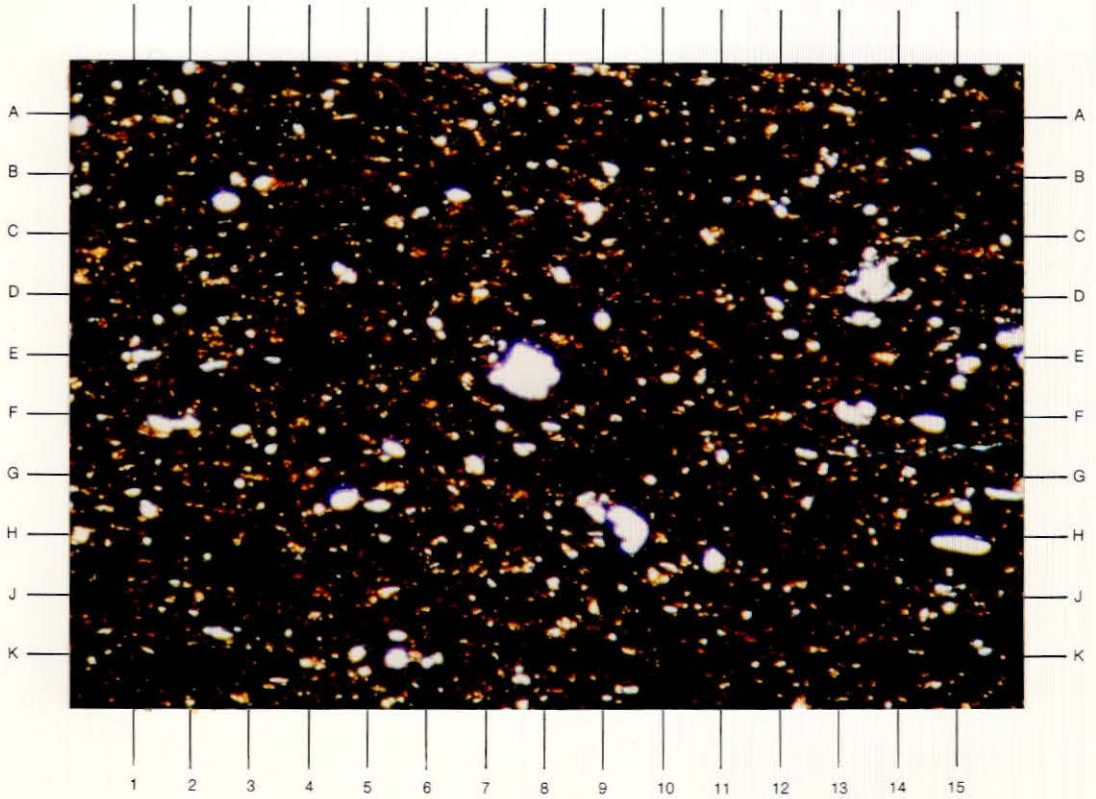

B

CORE LABORATORIES, INC.

Reservoir Geology/Petrographic Services

SCANNING ELECTRON MICROSCOPY

PHOTOMICROGRAPHS AND DESCRIPTIONS

Symbols appear at the bottom of all SEM photomicrographs in this report. From left to right, these are: 20Kv (SEM electron accelerating potential, kilovolts), magnification (X1000), bar scale (microns), and photograph exposure number.

Core Research, Inc. File: 186216

Sample Number: 28G-1

Plate 5A

This low-magnification photomicrograph shows a view taken perpendicular to the fissile layers. Heterogeneously distributed, silt-size particles of quartz, feldspar (C5), and muscovite comprise the siliciclastic debris. These silt-size particles are set in a matrix composed of detrital and/or recrystallized clays, organic material, and finely divided aggregates of pyrite. No visible porosity is present in this view. (40X)

Plate 5B

An albite (B8) particle partially coated by poorly defined clay is shown in this high-magnification view. Analyses by Energy Dispersive Spectroscopy (EDS) reveal the present of silicon (Si), aluminum (Al), potassium (K), and iron (Fe). These clays do not appear to be one clay type, such as mixed-layer illite/smectite, but rather a combination of different clays. Abundant, ineffective microporosity is associated with these clays. (1310X)

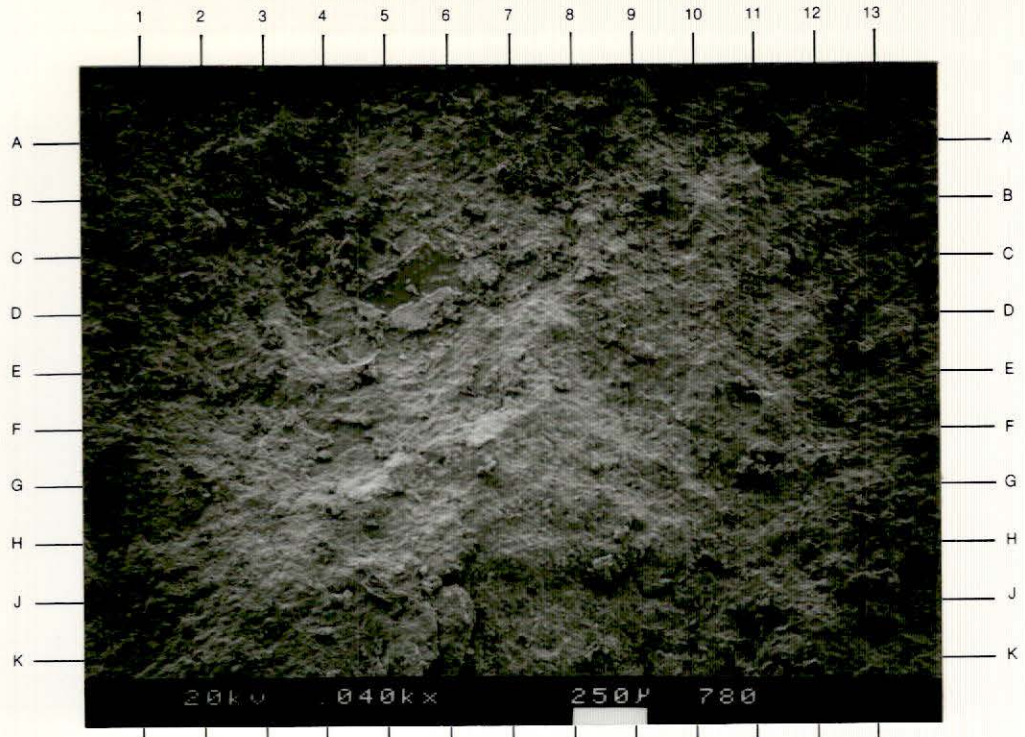

A

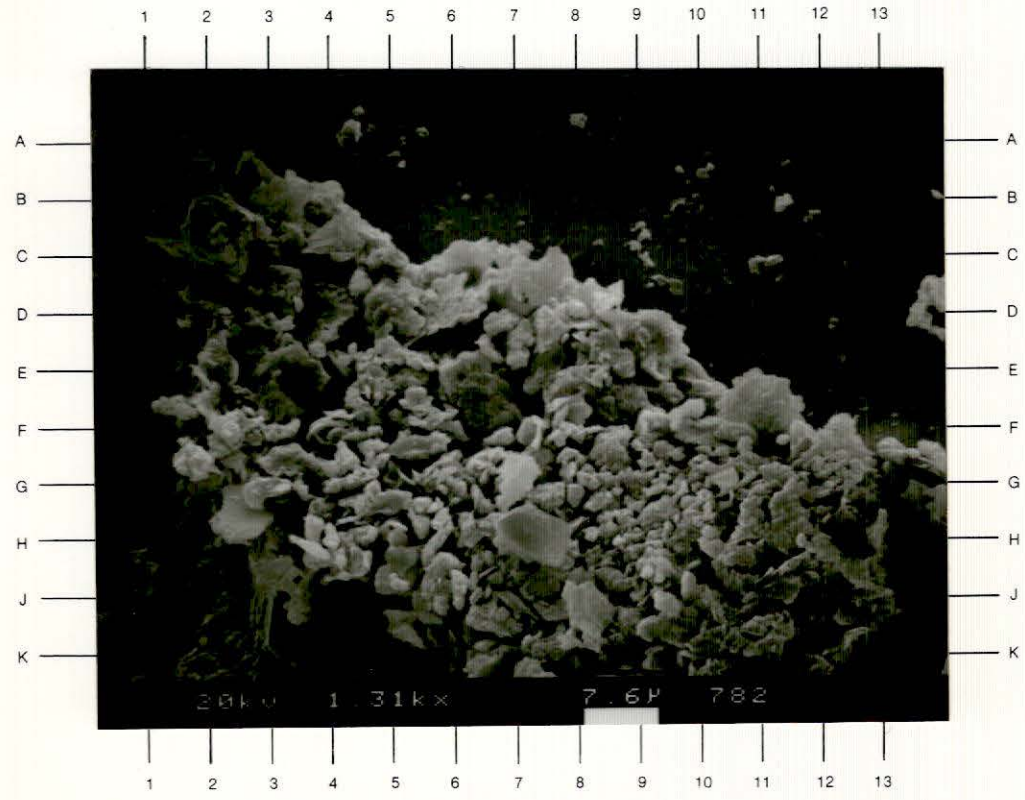

B

CORE LABORATORIES, INC.

Reservoir Geology/Petrographic Services

Core Research, Inc. File: 186216

Sample Number: 28G-1

Plate 6A

This image, taken using the back-scatter detector, shows a delaminated muscovite flake (E6) set in poorly defined matrix material. Scattered quartz (H4) and potassium feldspar (B10) particles are also observed. The majority of the view is occupied by poorly defined detrital to partially recrystallized clayey matrix material. EDS analyses reveal that the matrix material at A1 is composed of aluminum (Al) and silicon (Si), both constituents of kaolinite. Poorly defined, but discernible, pseudohexagonal outlines are shown by the individual platelets comprising this aggregate. The fissile character of this sample is evident at G1 and G10. (1500X)

Plate 6B

Another view of the sample highlights the presence of Fe-dolomite (C4, F4, F7, H4). This authigenic mineral occurs as a replacement of either matrix material or silt-size particles. The fissile character of the clayey matrix material is evident at A8, C7, and D13. A former particle site is shown at A1. (3000X)

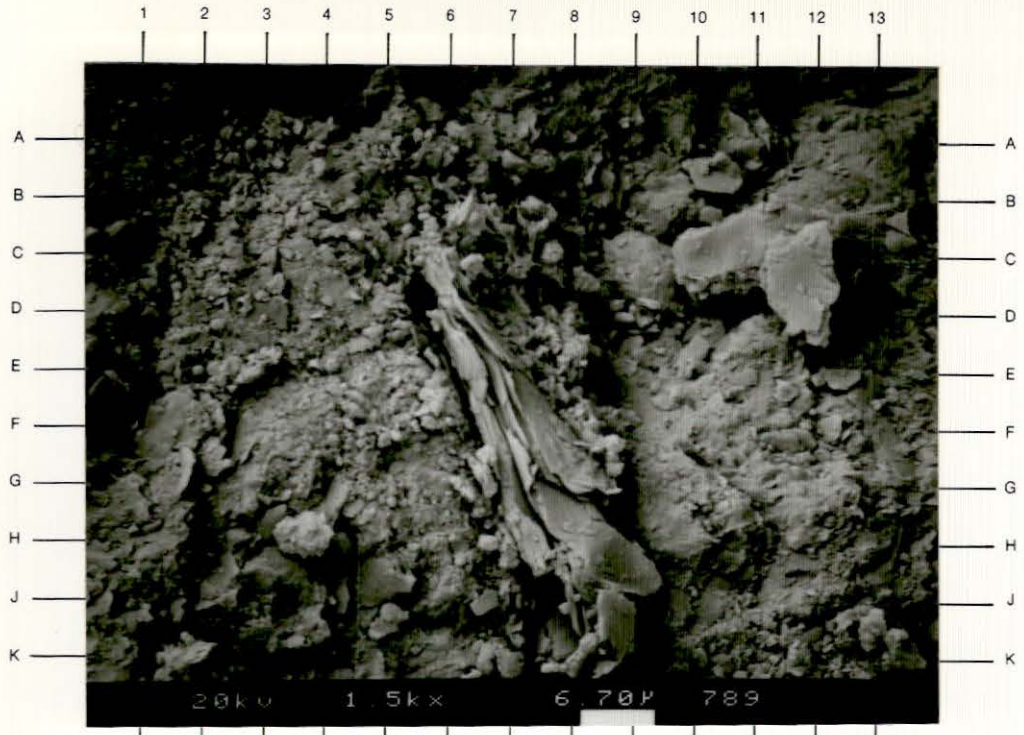

A

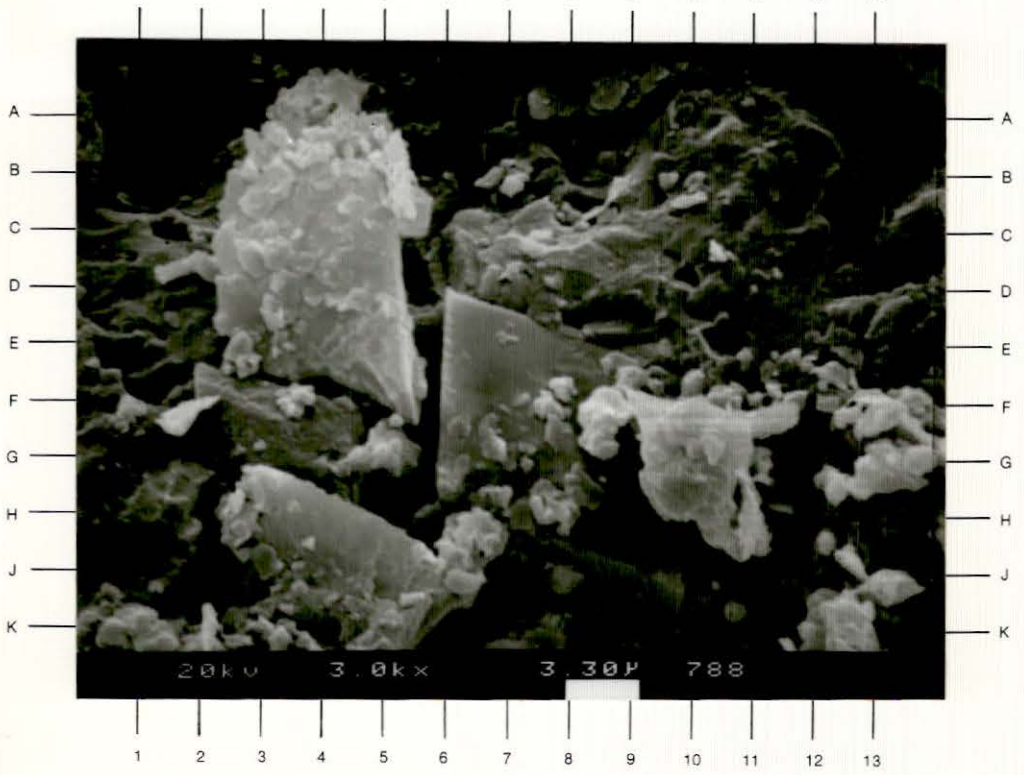

B

CORE LABORATORIES, INC.

Reservoir Geology/Petrographic Services

Core Research, Inc. File: 186216

Sample Number: 28G-2

Plate 7A

A low-magnification back-scatter image of the sample reveals a fissile, laminated shale. Silt-size particles include quartz, feldspar, and muscovite. Detrital to partially recrystallized clay minerals, organic material, and pyrite comprise the matrix material. The lighter gray areas of this view (D6, D11-12, G6) highlight areas rich in pyrite. Some fractures (C8, E3-4, H12) were induced during sample preparation. (40X)

Plate 7B

A more detailed view of the sample shows the poorly defined matrix material that comprises most of this sample. EDS analysis reveals the presence of abundant silicon (Si), aluminum (Al), and potassium (K). These three elements are constituents of illite, indicating that the matrix material in this view may be primarily illitic. A quartz particle occurs at F-G9. (880X)

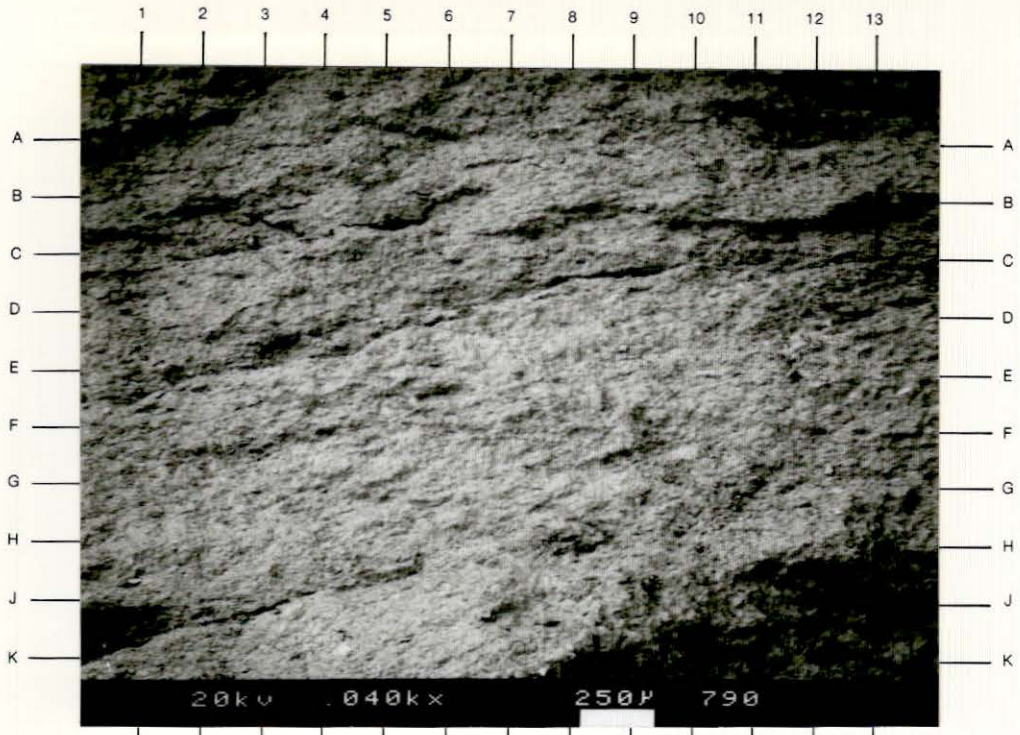

A

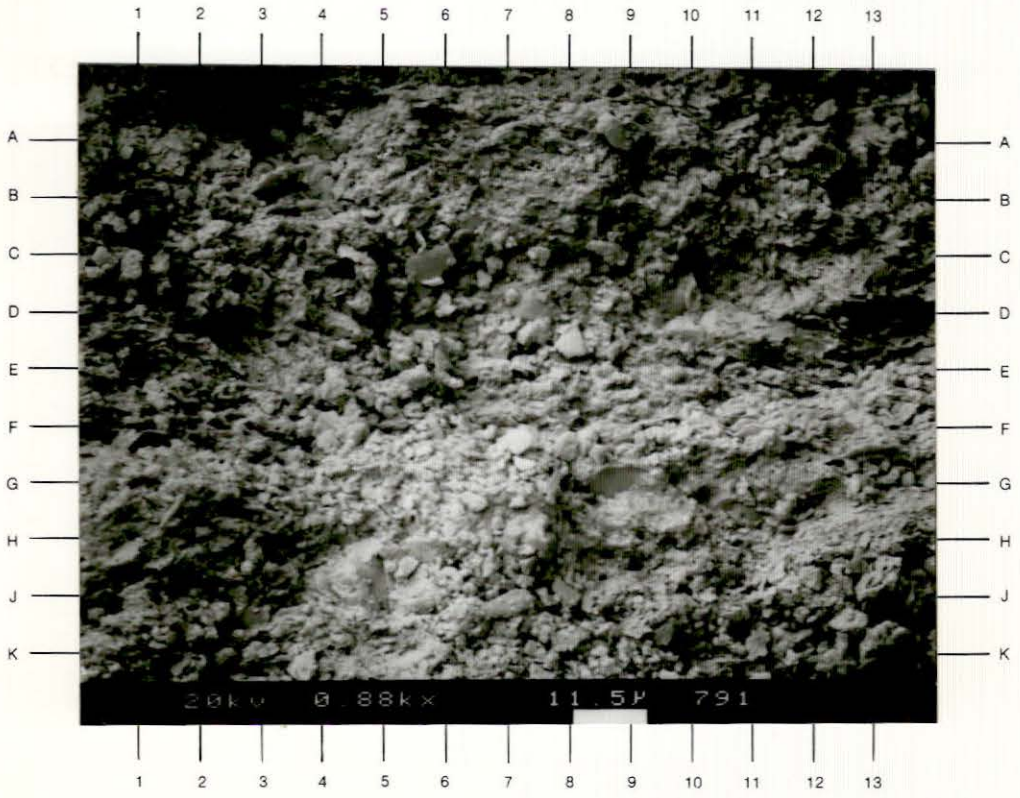

B

CORE LABORATORIES, INC.

Reservoir Geology/Petrographic Services

Sample Number: 28G-2

Plate 8A

Another view of the sample provides a closer look at the matrix material. The matrix consists of a series of compacted clay flakes in subparallel to parallel alignment. No distinctive morphology is displayed by these clay flakes; however, EDS analyses reveal the presence of silicon (Si), aluminum (Al), potassium (K), magnesium (Mg), and iron (Fe). These elements may be present in either a mixed-layer illite/smectite or may be present as components of several different, mechanically mixed, clay minerals. (2000X)

Plate 8B

The parallel alignment of the clay flakes (E11, G6, H8) is clearly displayed in this view. Detrital quartz (H4) and albite (K11) particles have been enveloped by the abundant clayey matrix. Numerous, but ineffective, micropores (F-G5-6) are associated with this clayey matrix. (3000X)

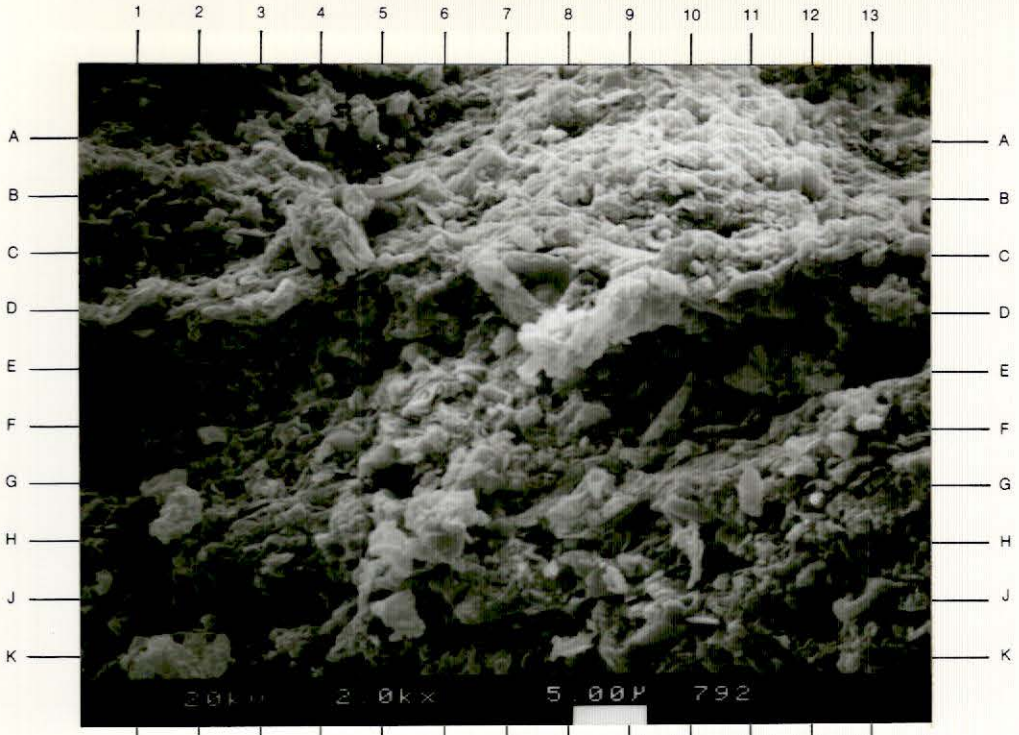

A

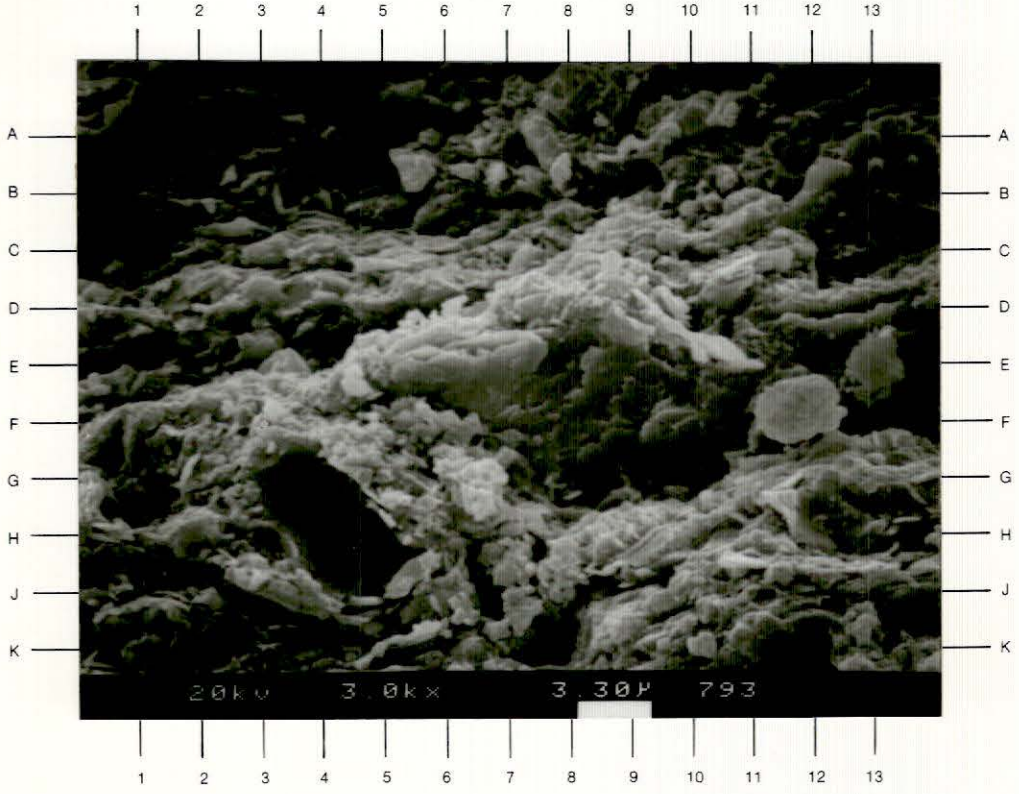

B

CORE LABORATORIES, INC.

Reservoir Geology/Petrographic Services

Core Research, Inc. File: 186216

Sample Number: 28G-3

Plate 9A

This low magnification view shows the surface of fissile layer in a planar-laminated shale. Poorly defined clayey matrix intermixed with organic material and pyrite are the dominant constituents of this sample. Heterogeneously, distributed quartz, feldspar, and muscovite particles are also present. Authigenic dolomite and pyrite occur as matrix and/or particle replacement minerals. No visible porosity is observed in this view. (40X)

Plate 9B

Another view of the sample focuses upon the matrix material. The parallel alignment of the clay flakes is clearly shown at A8, C12, and C13. Pyrite (D4, H-J4, G13) is intermixed with the poorly defined clay minerals that comprise this sample. (2000X)

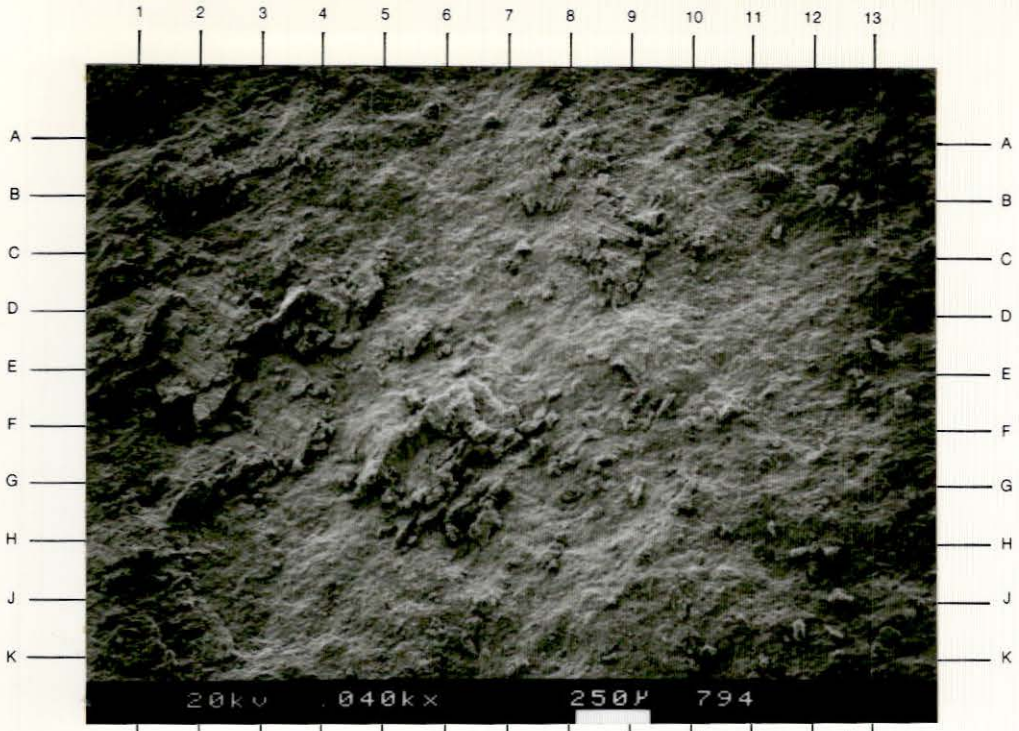

A

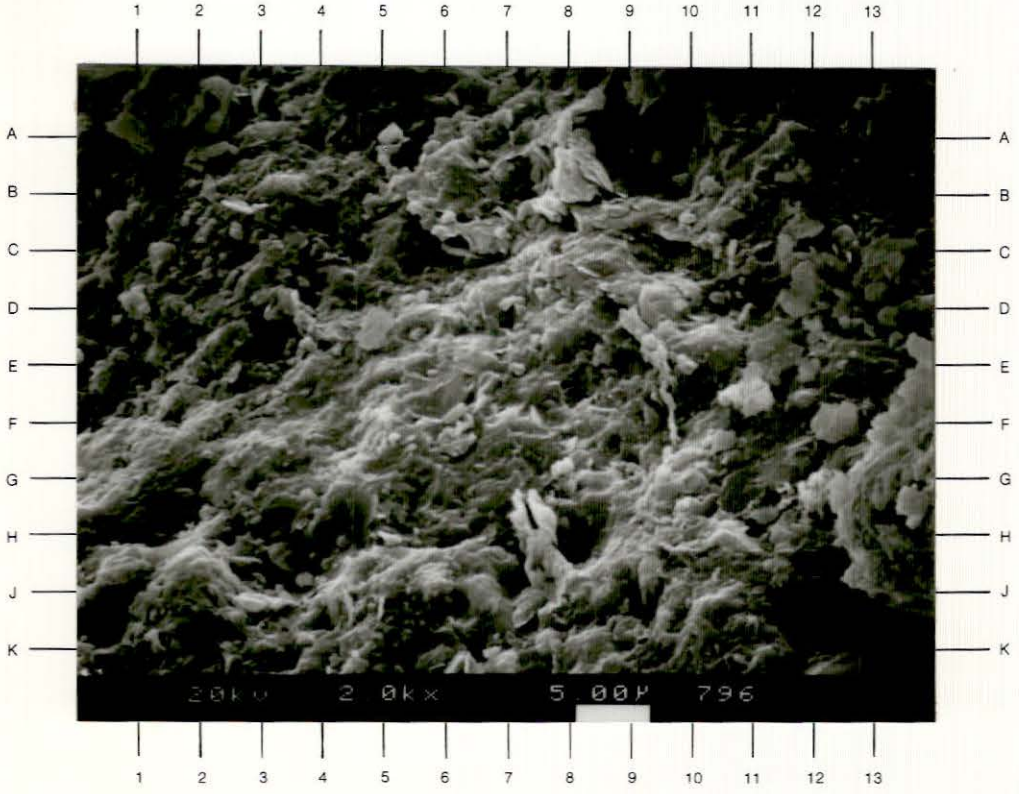

B

CORE LABORATORIES, INC.

Reservoir Geology/Petrographic Services

Sample Number: 28G-3

Plate 10A

A detrital biotite flake (F7) is shown in this high-magnification photomicrograph. The biotite flake is surrounded by platy clay flakes with lath-like extensions (E6-7). These lath-like extensions are characteristic of illite. EDS analysis confirms the presence of silicon (Si), aluminum (Al), and potassium (K), all essential elements of illite. A feldspar particle occurs at D2. (2500X)

Plate 10B

Another high-magnification image reveals the presence of calcite (C11) and a sulphate mineral [gypsum(?), J8-9]. These two authigenic minerals occur as matrix and/or silt-size particle replacement minerals. The calcite crystals in this view display subhedral outlines. Pyrite can be observed at B9 and F6. Poorly defined, flaky clay minerals occupy the remainder of the view. EDS analyses reveal the presence of silicon (Si), aluminum (Al), and potassium (K), all constituents of illite. (2500X)

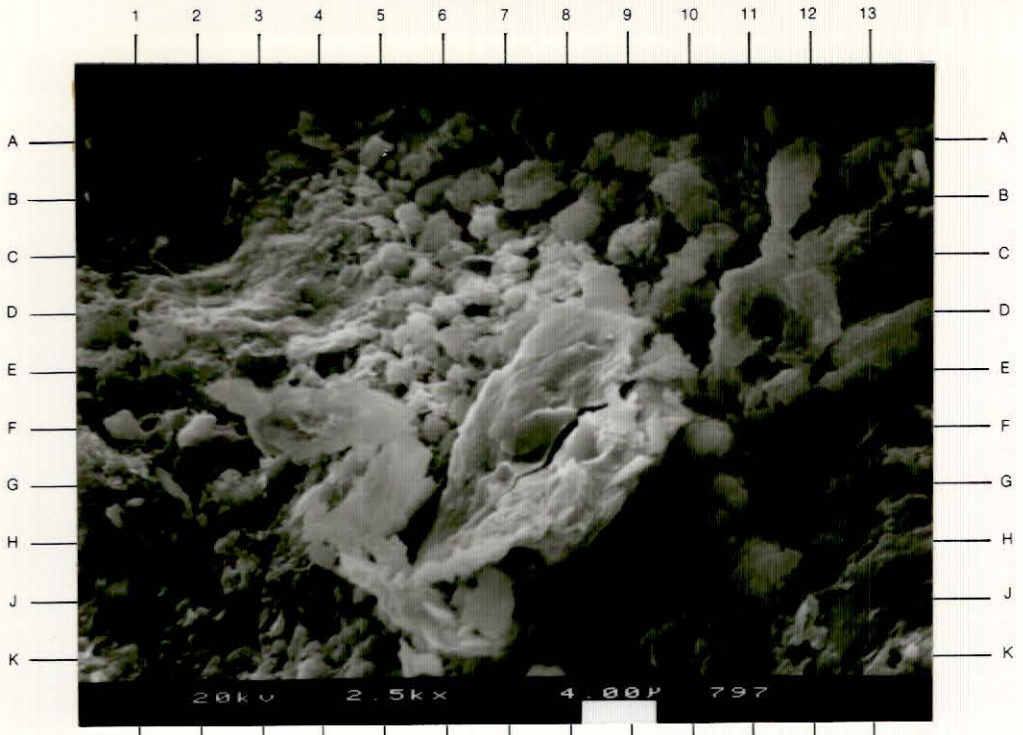

A

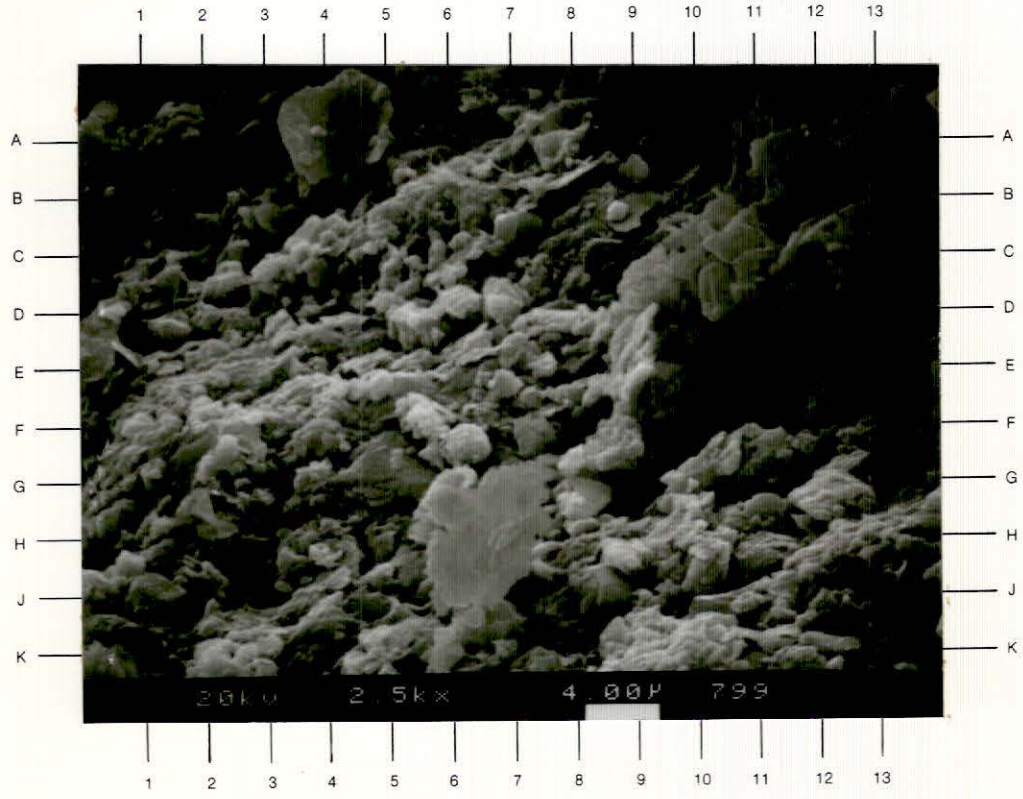

B

CORE LABORATORIES, INC.

Reservoir Geology/Petrographic Services

Core Research, Inc. File: 186216

Sample Number: 28G-4

Plate 11A

This photomicrograph shows a general view of the sample taken perpendicular to the fissile, planar laminae present in this shale. Silt-size particles of quartz, feldspar, and muscovite are enveloped by clayey matrix material, pyrite, and organic material. Scattered patches of authigenic dolomite and calcite are also observed. No visible porosity was noted in this view. (40X)

Plate 11B

A former particle site (A2 through A11) is shown in this view. This former particle site is surrounded by authigenic silica cement, as shown by the smooth surfaces at C8, F3, and F7. Poorly defined, detrital clay flakes (A5, C6) were compacted between the authigenic silica and the particles. (2000X)

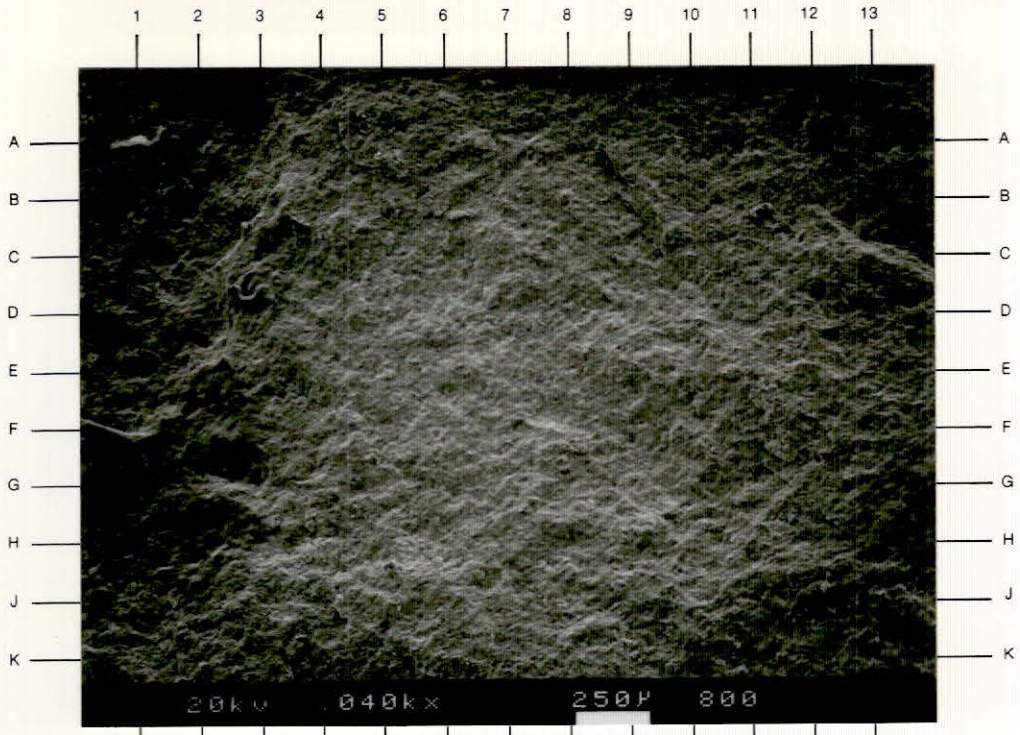

A

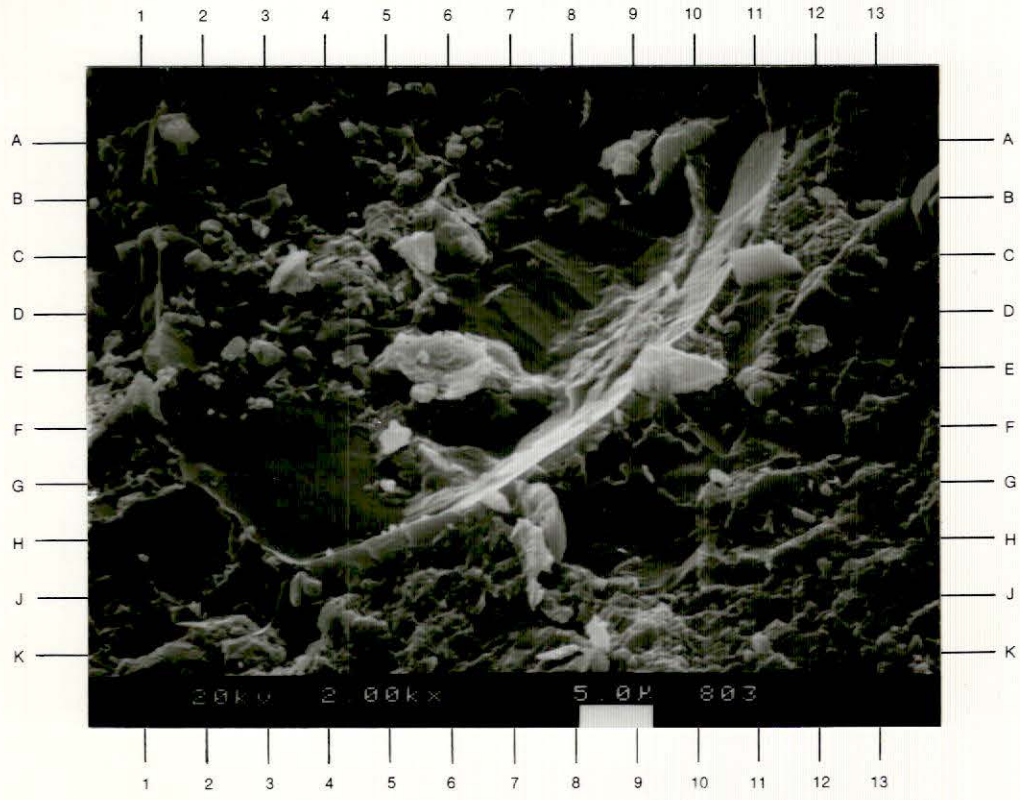

B

CORE LABORATORIES, INC.

Reservoir Geology/Petrographic Services

Sample Number: 28G-4

Plate 12A

The fissile layering present in this shale is clearly shown in this high-magnification image. Minor recrystallization of the clayey matrix material has occurred at B3 and J11. These recrystallized clays display the webby/hairy morphology characteristic of mixed-layer illite/smectite. Quartz (D11) and plagioclase feldspar (K5) can be observed in this view. Abundant, noneffective microporosity is associated with the clayey matrix material. (2000X)

Plate 12B

This high-magnification photomicrograph shows an authigenic potassium feldspar crystal (D5) surrounded by poorly defined detrital matrix material (E6, B10). Pyrite crystals occur at C6 and A7-8. The pyrite crystals at A7-8 partially coat the secondary quartz overgrowth at B7-8. A pyrite framboid can be noted at G1. (2500X)

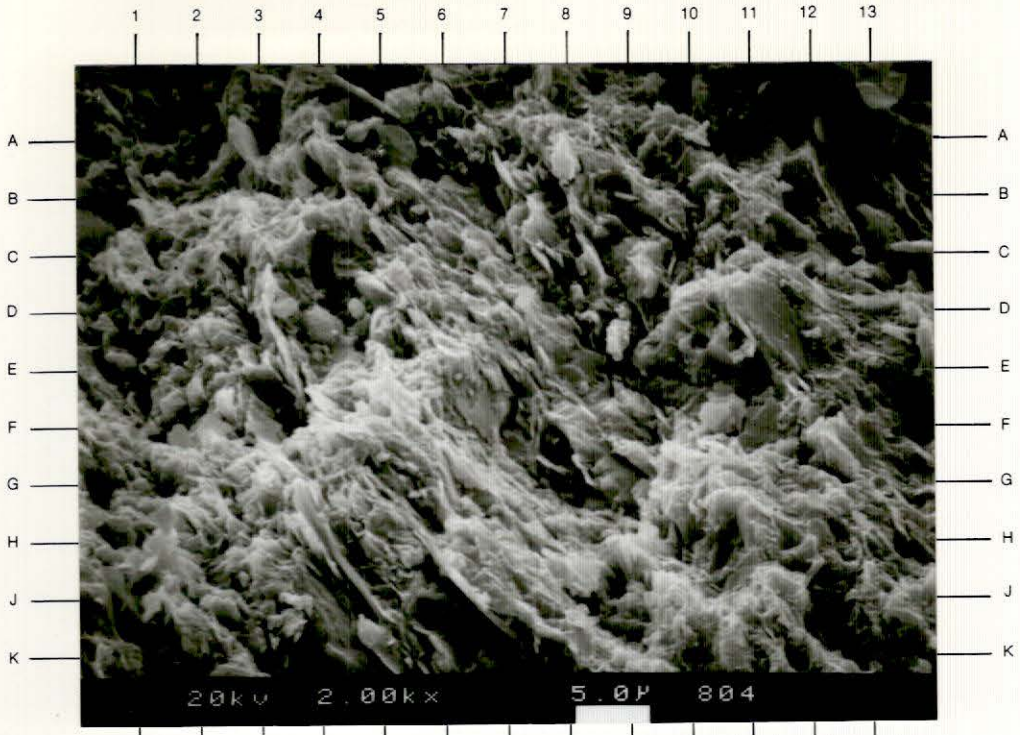

A

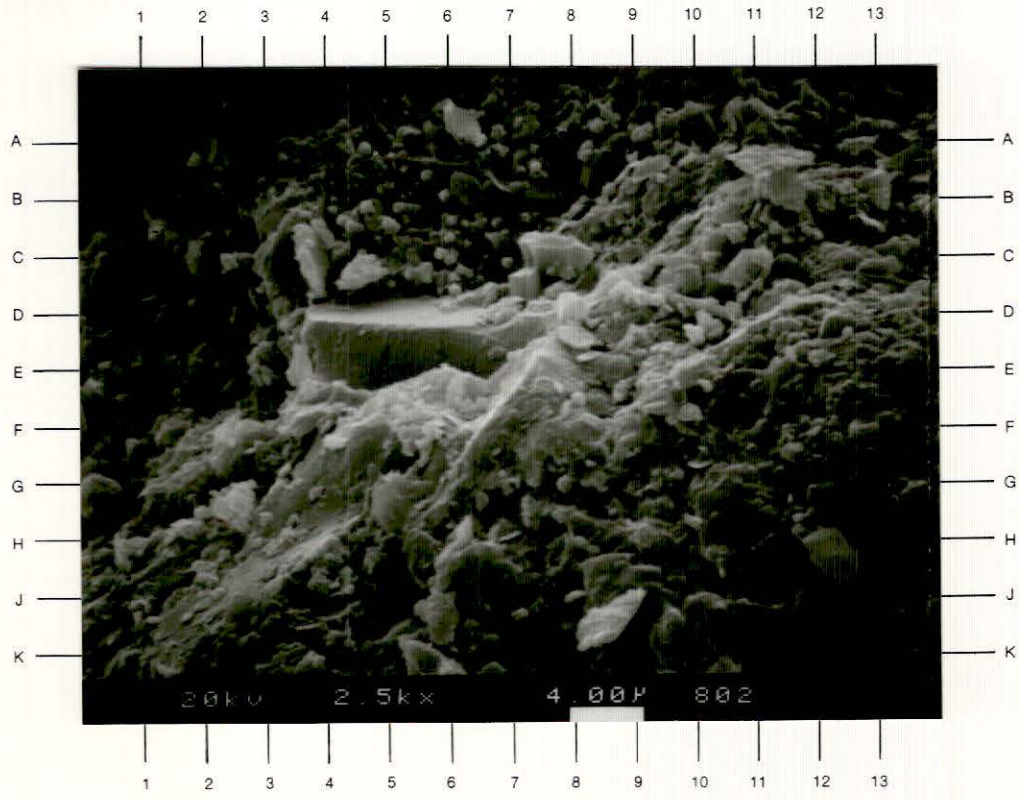

B

CORE LABORATORIES, INC.

Reservoir Geology/Petrographic Services

VOLUME II
PART III

GEOCHEMISTRY

T A B L E O F C O N T E N T S

S U M M A R Y

Four (4) core samples were analyzed for kerogen composition and vitrinite reflectance. The sample depths are as follows:

I.D. No.	Depth (ft)
EM 18-22-1	7137.1
EM 18-22-2	7141.7
EM 18-22-3	7147.7
EM 18-22-4	7153.4

The subject samples all contain significant amounts of `woody' material that is thermally post mature. The kerogen data summary (Table 1, Part III) indicates that 90 to 100 percent of the identified kerogen is this woody material. This material is considered to be gas prone as opposed to other kerogen types, such as algal/amorphous material, that are considered oil prone. Between a trace and 10 percent of amorphous kerogen was identified. Because of the small size of a majority of the vitrinite present, only a small percentage could be recorded for the mean vitrinite reflectance values. The number of readings of `indigenous population' (see Figures 1 through 4, Part III) range from 12 to 16. This is somewhat marginal for meaningful statistics. However, the overall interpretation that these data reflect thermally post mature kerogen is probably sound.

TABLE 1. KEROGEN DATA SUMMARY

Well Name: Eda McLain No. 18-22
Location: Upshur County, West Virginia

I.D. No.	Depth (ft)	Percent Amorphous	Percent Exinite	Percent Woody	Percent Inertinite	Thermal Alteration Index (TAI)	Vitrinite Reflectance	Remarks
EM-18-22-1	7137.1	10		90		4	1.79*	
EM-18-22-2	7141.7	5		95		4	2.00*	
EM-18-22-3	7147.7	T		100		4	1.97*	
EM-18-22-4	7153.4	T		100		4	1.94*	

Amorphous = algal debris + amorphous sapropels; Exinite = waxy and resinous materials generally having a characteristic form; i.e., plant cuticle, pollen, spores, resins, etc.

* Insufficient vitrinite for an accurate R_o determination.

Figure 1

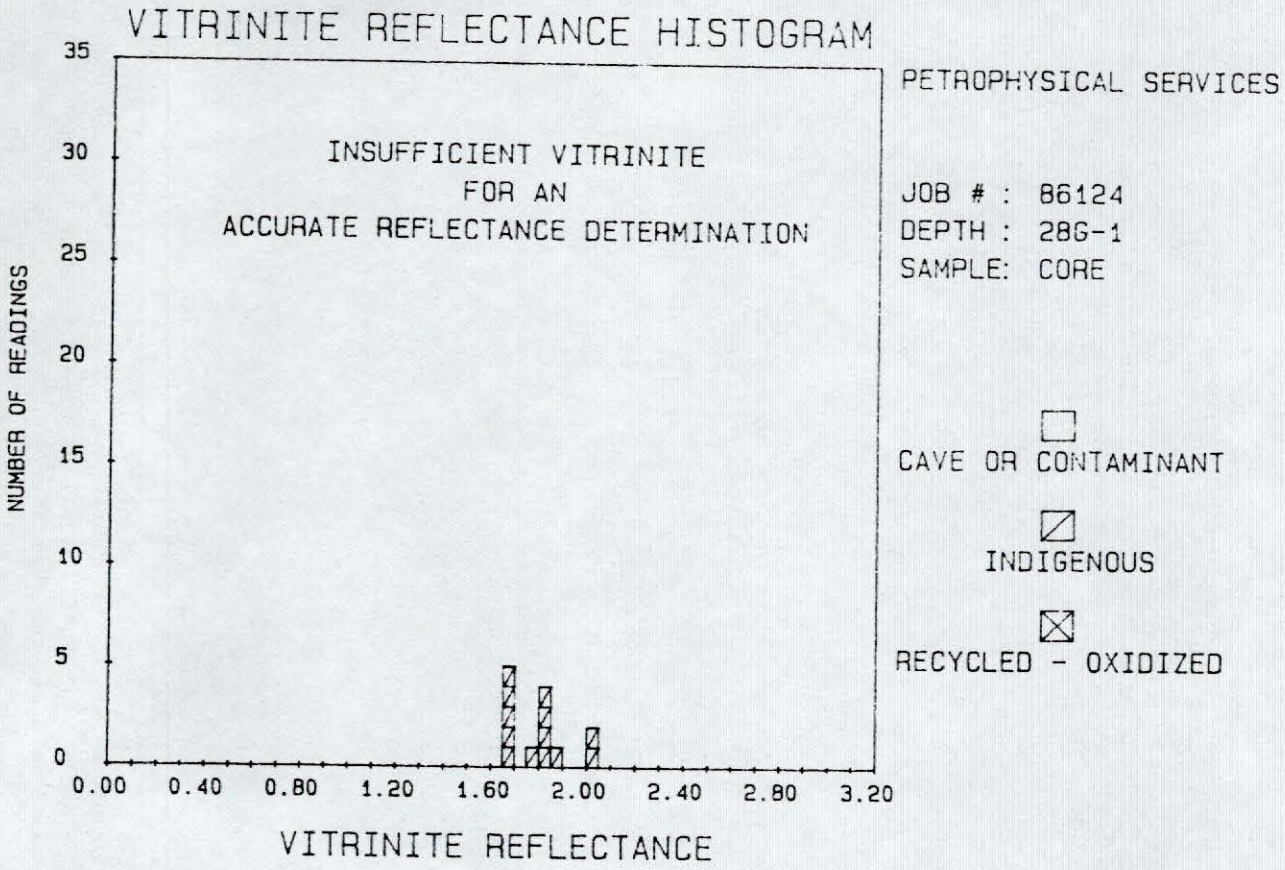

STATISTICS FOR THE INDIGENOUS POPULATION

NUMBER OF READINGS	13	STANDARD DEVIATION	0.47
MEAN REF.	1.79 %	MEDIAN	1.80
MIN. REF.	1.66 %	MODE	1.69
MAX. REF.	2.01 %	SKEWNESS	-0.03

STATISTICS FOR THE TOTAL POPULATION

	READINGS		PERCENT OF POPULATION
CAVE OR CONTAMINANT	0	CAVE OR CONTAMINANT	0.0 %
INDIGENOUS	13	INDIGENOUS	100.0 %
RECYCLED - OXIDIZED	0	RECYCLED - OXIDIZED	0.0 %
TOTAL	13	TOTAL	100.0 %

Figure 2

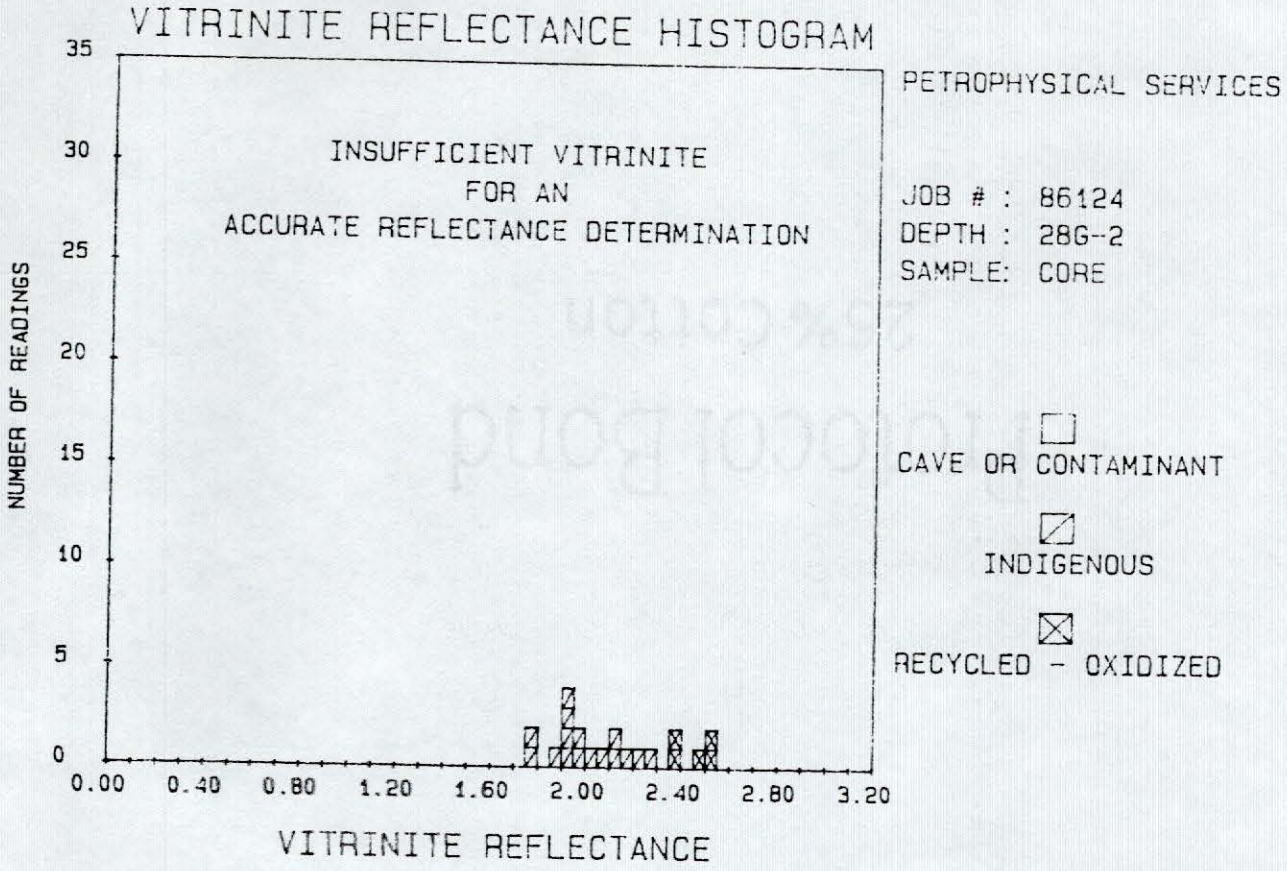

STATISTICS FOR THE INDIGENOUS POPULATION

NUMBER OF READINGS	16	STANDARD DEVIATION	0.25
MEAN REF.	2.00 %	MEDIAN	2.00
MIN. REF.	1.79 %	MODE	1.79
MAX. REF.	2.25 %	SKEWNESS	-0.02

STATISTICS FOR THE TOTAL POPULATION

	READINGS		PERCENT OF POPULATION
CAVE OR CONTAMINANT	0	CAVE OR CONTAMINANT	0.0 %
INDIGENOUS	16	INDIGENOUS	76.2 %
RECYCLED - OXIDIZED	5	RECYCLED - OXIDIZED	23.8 %
TOTAL	21	TOTAL	100.0 %

Figure 3

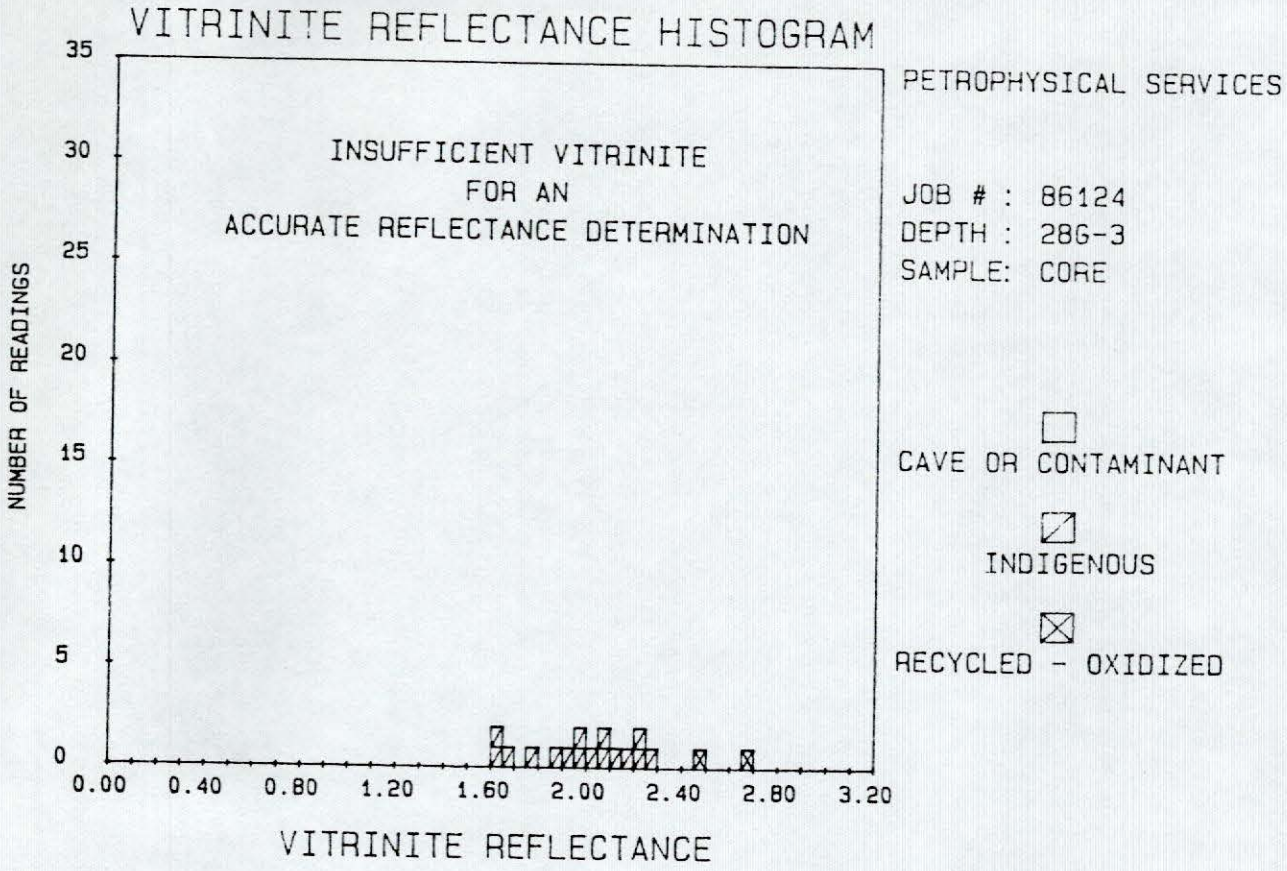

STATISTICS FOR THE INDIGENOUS POPULATION

NUMBER OF READINGS	16	STANDARD DEVIATION	0.28
MEAN REF.	1.97 %	MEDIAN	1.97
MIN. REF.	1.61 %	MODE	1.96
MAX. REF.	2.26 %	SKEWNESS	-0.03

STATISTICS FOR THE TOTAL POPULATION

	READINGS		PERCENT OF POPULATION
CAVE OR CONTAMINANT	0	CAVE OR CONTAMINANT	0.0 %
INDIGENOUS	16	INDIGENOUS	88.9 %
RECYCLED - OXIDIZED	2	RECYCLED - OXIDIZED	11.1 %
TOTAL	18	TOTAL	100.0 %

Figure 4

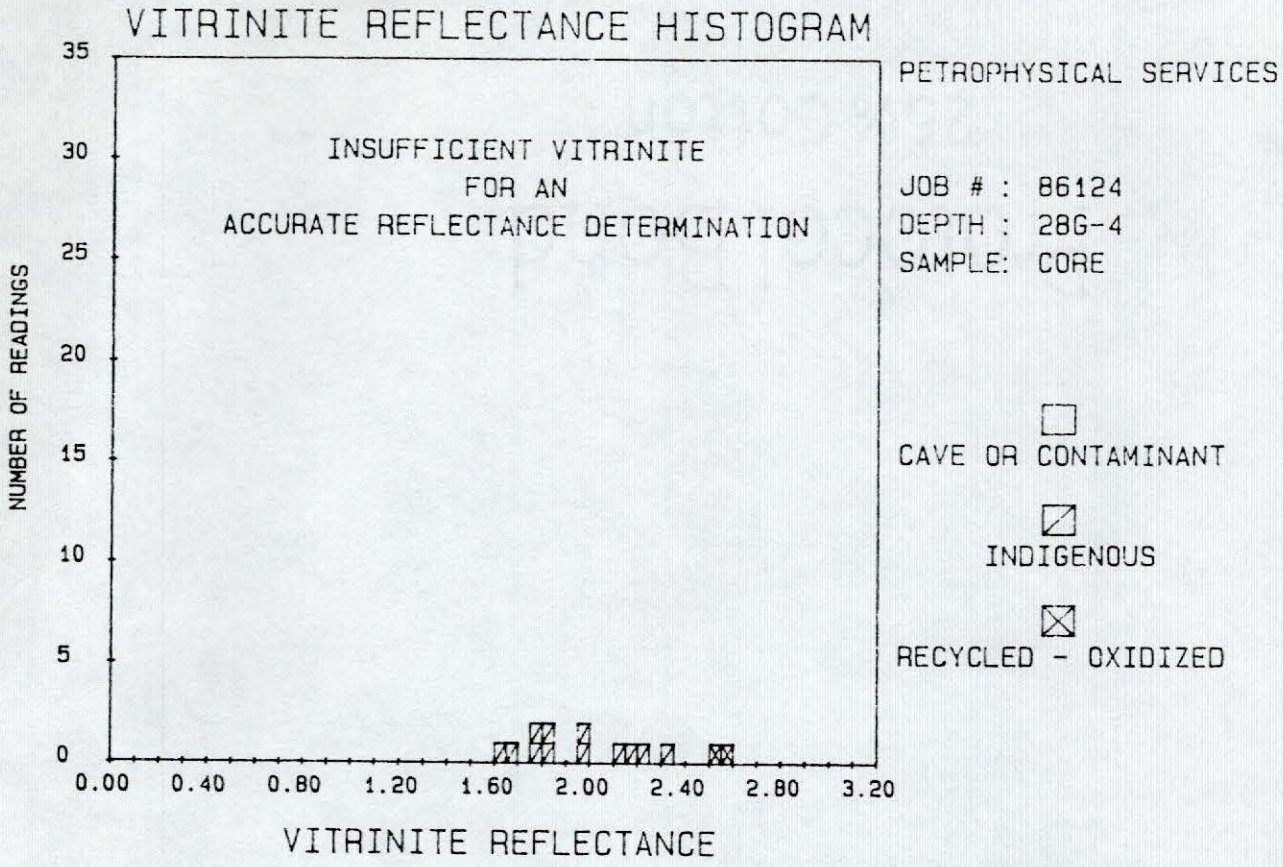

STATISTICS FOR THE INDIGENOUS POPULATION

NUMBER OF READINGS	12	STANDARD DEVIATION	0.07
MEAN REF.	1.94 %	MEDIAN	1.94
MIN. REF.	1.63 %	MODE	1.63
MAX. REF.	2.34 %	SKEWNESS	-0.04

STATISTICS FOR THE TOTAL POPULATION

	READINGS		PERCENT OF POPULATION
CAVE OR CONTAMINANT	0	CAVE OR CONTAMINANT	0.0 %
INDIGENOUS	12	INDIGENOUS	85.7 %
RECYCLED - OXIDIZED	2	RECYCLED - OXIDIZED	14.3 %
TOTAL	14	TOTAL	100.0 %